UNIVERSITY OF CRETE

MSc "OPTICS & VISION"

MSc dissertation:

"Evaluating threshold and supra-threshold performance using compound gratings"

Athanasios Panorgias

Supervisor: Dr Sotiris Plainis

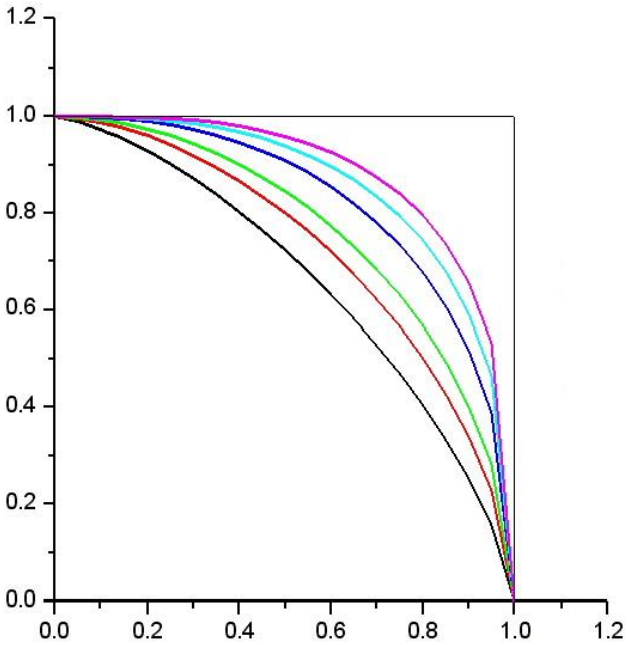

Heraklion, 2007

UNIVERSITY OF CRETE

MSc "OPTICS & VISION"

MSc dissertation:

"Evaluating threshold and supra-threshold performance using compound gratings"

Athanasios Panorgias

Supervisor: Dr Sotiris Plainis

This study was submitted as part of the obligations for the conferment of the Master in Science certification of the MSc Program "Optics and Vision" and was presented at the three-member committee constituted by:

1) Dr Sotiris Plainis
2) Dr Ian Murray
3) Dr Neil Parry

Heraklion, 2007

ΥΠΟΥΡΓΕΙΟ ΕΘΝΙΚΗΣ ΠΑΙΔΕΙΑΣ ΚΑΙ ΘΡΗΣΚΕΥΜΑΤΩΝ
ΕΙΔΙΚΗ ΥΠΗΡΕΣΙΑ ΔΙΑΧΕΙΡΙΣΗΣ ΕΠΕΑΕΚ
ΕΥΡΩΠΑΪΚΗ ΕΝΩΣΗ
ΣΥΓΧΡΗΜΑΤΟΔΟΤΗΣΗ
ΕΥΡΩΠΑΪΚΟ ΚΟΙΝΩΝΙΚΟ ΤΑΜΕΙΟ
Η ΠΑΙΔΕΙΑ ΣΤΗΝ ΚΟΡΥΦΗ
Επιχειρησιακό Πρόγραμμα
Εκπαίδευσης και Αρχικής
Επαγγελματικής Κατάρτισης
ΕΛΛΑΔΑ 2008
Ανάπτυξη παντού. Ανάπτυξη για όλους.

ABSTRACT

Most of the understanding regarding visual contrast perception has been achieved using simple gratings, which stimulate spatially tuned neuronal mechanisms. In order to study any interaction between these channels more elaborated stimuli need to be used. The incentive of the present study was to assess the contrast sensitivity using a wide range of spatial frequencies at the high spatial frequency side of the contrast sensitivity function. The description of the form and the extent of the underlying mechanisms of the human visual system was another issue studies in the present work. Moreover, their recognition was evaluated at sub-threshold and supra-threshold combinations.

Methodology

For the experiments a high resolution FD Trinitron® SONY© GDM F520 CRT monitor, a VSG 2/5 (Cambridge Research Systems©) graphic card, a CB6 wireless remote control (Cambridge Research Systems©) and a specially developed software for stimuli generation (NewRT, Dr Neil Parry©) were used. Five observers, all with prior psychophysical experience, participated in the experiments.

Three sets of experiments were conducted. The first two experiments were designed to evaluate threshold performance of compound gratings. The main spatial frequency component was always 4c/deg and the spatial frequency of the secondary component was 4.5, 5, 6, 8, 12, 16 and 24 which corresponds at a spatial frequency ratio of 1.125, 1.25, 1.5, 2, 3, 4 and 6. The third experiment was conducted to examine the interaction between the spatial frequency tuned channels while the contrast of the two components of the compound gratings ranged from sub-threshold to supra-threshold.

Results

Compound gratings were found to be slightly more sensitive by a factor of x1.15 (which corresponds to an average 1.2dB difference) compared to

the sensitivity of individual gratings (while the two components were at equal contrast above their respective thresholds). For spatial frequency ratio equal to one (the components were of same frequency), the sensitivity was higher (compared to the single grating) by 6dB (maximum summation), decreasing to 2-4 dBs for ratios between 1 and 2. When the spatial frequency ratio was > 2 there were no channel interactions and the sensitivity is solely increased due to probability summation, by a factor between 1.15 and 1.345.

The bandwidth of the spatial frequency tuned channel selective at 4c/deg was found to be at FWHM about 0.4 to 0.6 octaves for the two subjects. Moreover, when the secondary component was of spatial frequency lower than 4c/deg, the magnitude of neuronal summation was higher, suggesting a non-symmetric neuronal channel.

When the two components were at supra-threshold contrast, the high spatial frequency component depresses the low spatial frequency component and appears more detectable.

Discussion

Compound gratings appear more detectable. The amount of increased sensitivity depends on the ratio between the spatial frequencies of the components, being maximum (6dB), when the components are of equal spatial frequency, decreasing to 2-4 dBs when the ratio is about 2. The increased sensitivity is due to neuronal summation. For ratios higher than 2 the sensitivity is increased about 1-2dB, corresponding to probability summation. There is evidence for asymmetric spatial-frequency tuned neuronal channels. Finally, there are indications that the high spatial frequency component is more detectable when the two components are at supra-threshold contrast.

ΠΕΡΙΛΗΨΗ

Η ερμηνεία της ευαισθησίας φωτεινής αντίθεσης έχει επιτευχθεί με τη χρησιμοποίηση απλών gratings που διεγείρουν μερικώς συντονισμένους νευρικούς μηχανισμούς. Προκειμένου να μελετηθούν αλληλεπιδράσεις μεταξύ τέτοιων καναλιών πρέπει να χρησιμοποιηθούν πιο περίπλοκα ερεθίσματα. Το κίνητρο για την πραγματοποίηση της παρούσας εργασίας ήταν να προσεγγίσει την ευαισθησία φωτεινής αντίθεσης χρησιμοποιώντας ευρύ φάσμα χωρικών συχνοτήτων από τη μεριά των υψηλών χωρικών συχνοτήτων της καμπύλης ευαισθησίας φωτεινής αντίθεσης. Η περιγραφή του σχήματος και του μεγέθους των υποκείμενων μηχανισμών του οπτικού συστήματος ήταν ένα άλλο θέμα το οποίο μελετήθηκε σε αυτή την εργασία. Επιπλέον, αξιολογήθηκε η αναγνωρισημότητά τους σε sub-threshold και supra-threshold συνδυασμούς contrast.

Μεθοδολογία

Για τα πειράματα χρησιμοποιήθηκαν μια οθόνη υψηλής ανάλυσης FD Trinitron® SONY© GDM F520 CRT, μια κάρτα γραφικών VSG 2/5 (Cambridge Research Systems©), ένα ασύρματο τηλεχειριστήριο CB6 (Cambridge Research Systems©) και ένα ειδικά σχεδιασμένο για παραγωγή οπτικών ερεθισμάτων λογισμικό (NewRT, Dr Neil Parry©). Οι παρατηρητές που συμμετείχαν στα πειράματα ήταν 5, όλοι με πρότερη εμπειρία σε ψυχοφυσικές μετρήσεις

Τρία πειράματα διεξήχθησαν. Τα πρώτα δυο σχεδιάστηκαν για να αξιολογηθεί η απόδοση του οπτικού συστήματος χρησιμοποιώντας σύνθετα gratings σε threshold contrast. Η κύρια χωρική συχνότητα ήταν πάντα 4c/deg ενώ η χωρική συχνότητα του δευτερεύοντος grating ήταν 4.5, 5, 6, 8, 12, 16, 24c/deg που αντιστοιχεί σε λόγο χωρικών συχνοτήτων 1.125, 1.25, 1.5, 2, 3, 4, 6. Το τρίτο πείραμα σχεδιάστηκε για να εξεταστεί η συσχέτιση μεταξύ νευρώνων καθώς η φωτεινή αντίθεση των δυο συνιστωσών του σύνθετου grating έπαιρνε τιμές τόσο μικρότερες όσο και μεγαλύτερες τις ουδούς.

Αποτελέσματα

Τα σύνθετα gratings βρέθηκαν να εμφανίζουν ελαφρώς πιο αυξημένη ευαισθησία από ότι τα απλά κατά έναν πολλαπλασιαστικό παράγοντα x1.15 (το οποίο σημαίνει διαφορά 1.2dB). Για λόγο χωρικών συχνοτήτων 1 (τα συνιστώσα gratings ήταν της ίδιας συχνότητας) η ευαισθησία ήταν αυξημένη (σε σχέση με τα απλά gratings) κατά 6dB (μέγιστη νευρωνική άθροιση) ενώ μειωνόταν σε 2-4dB για λόγο χωρικών συχνοτήτων μεταξύ 1 και 2. Όταν ο λόγος χωρικών συχνοτήτων ήταν μεγαλύτερος από 2 δεν υπήρχε νευρωνική αλληλεπίδραση και η ευαισθησία ήταν αυξημένη εξαιτίας μόνο του probability summation, κατά ένα παράγοντα μεταξύ 1.15 και 1.345.

Το εύρος του νευρωνικού καναλιού που εμφανίζει αυξημένη ευαισθησία στη χωρική συχνότητα των 4 κύκλων ανά μοίρα μετρήθηκε στο FWHM και βρέθηκε να είναι μεταξύ 0.4 και 0.6 οκτάβων για 2 παρατηρητές. Επιπλέον, όταν η χωρική συχνότητα του δευτερεύοντος grating ήταν χαμηλότερη από 4c/deg το μέγεθος της νευρωνικής αλληλεπίδρασης ήταν υψηλότερο, υποδηλώνοντας ένα μη συμμετρικό νευρωνικό κανάλι.

Όταν τα δυο συνιστώσα gratings είχαν contrast πάνω από την ουδό, η υψηλής χωρικής συχνότητας συνιστώσα 'καταπιέζει' το grating χαμηλής χωρικής συχνότητας και εμφανίζεται περισσότερο ανιχνεύσιμο.

Συζήτηση

Τα σύνθετα gratings είναι περισσότερο ανιχνεύσιμα. Το εύρος της αυξημένης ευαισθησίας εξαρτάται από το λόγο των χωρικών συχνοτήτων των συνιστωσών τους και εμφανίζεται μέγιστη (6dB) όταν οι συνιστώσες έχουν την ίδια χωρική συχνότητα και μειώνεται σε 2-4dB όταν ο λόγος χωρικών συχνοτήτων είναι περίπου 2. Η αύξηση της ευαισθησίας οφείλεται σε νευρωνικές αλληλεπιδράσεις. Για λόγο χωρικών συχνοτήτων μεγαλύτερο από 2, η ευαισθησία είναι αυξημένη κατά 1-2dB, που αντιστοιχεί σε probability summation. Υπάρχουν στοιχεία ότι τα νευρωνικά κανάλια που είναι συντονισμένα σε χωρικές συχνότητες δεν είναι συμμετρικά. Τέλος, υπάρχουν

ενδείξεις ότι η συνιστώσα υψηλής χωρικής συχνότητας είναι περισσότερο ανιχνεύσιμη όταν και οι δυο συνιστώσες έχουν supra-threshold contrast.

Αφιερώνεται στην Μητέρα μου
και στον Πατέρα μου

I would like to express my sincere gratitude to my supervisor, Dr Sotiris Plainis for entrusting me to handle this issue, which was arisen with the assistance of his collaborators at the University of Manchester. His expert guidance and support at critical points have been extremely valuable for the completion of this study. I am also deeply grateful to him because he gave me the unique opportunity to experience the research process, as it is conduced at the universities abroad.

I must also acknowledge the other members of my committee, Dr Murray and Dr Parry for our excellent cooperation at the University of Manchester. Their assistance and direction during the whole research process have been of major importance for this study.

I wish to thank Triseugeni Giannakopoulou for her patient participation in the conduction of the experiments.

Finally, special thanks go out to all my dear friends who stand by me and keep faith in me all these years. . . .

Contents

Part of the experiments was conducted at
The University of Manchester

1.0 CHAPTER 1. INTRODUCTION

In this chapter a brief physiological overview of the visual system in higher primates is presented. The chapter begins with a description of the main neural components of the primary visual pathway between the eye and visual cortex. The optics of the eye and sub-cortical pathways are not discussed because are out of the purposes of this study. Next, an extensive overview of the spatial contrast sensitivity, which is a psychophysical method for evaluating visual performance, is presented. Also, we will refer to compound gratings, their mathematical formulas and final to theories about neural channels in human visual system.

1.1 Neurophysiology -The primary visual pathway

Although it is widely believe that we see with our eyes, this impression is erroneous. The organ which is responsible for our vision is the brain. For the purposes of the present study the eyes can be rewarded simply as an extension of the brain to the outer world. They are the organs which collect information and transmit it for further processing. For this reason, an introduction to the visual pathway is necessary.

The rays of light are collected by the optic elements of the eye and are focused to the outer layers of the retina. At this point light is absorbed by the pigment of the photoreceptors and converted to potential difference. These signals are transmitted to the ganglion cells and via the optic nerve, which exits the eye from the optic disk, the axons of the ganglion cells terminate in the LGN (Lateral Geniculate Nucleous), where a secondary process takes part. From the LGN, fibres ascend via the white matter and terminate in the Primary Visual Cortex (V1). Further processing of the information takes place in the higher visual centres such as V2, V3, where motion is analysed and V4 where colour is said to be analysed (see figure 1.1)

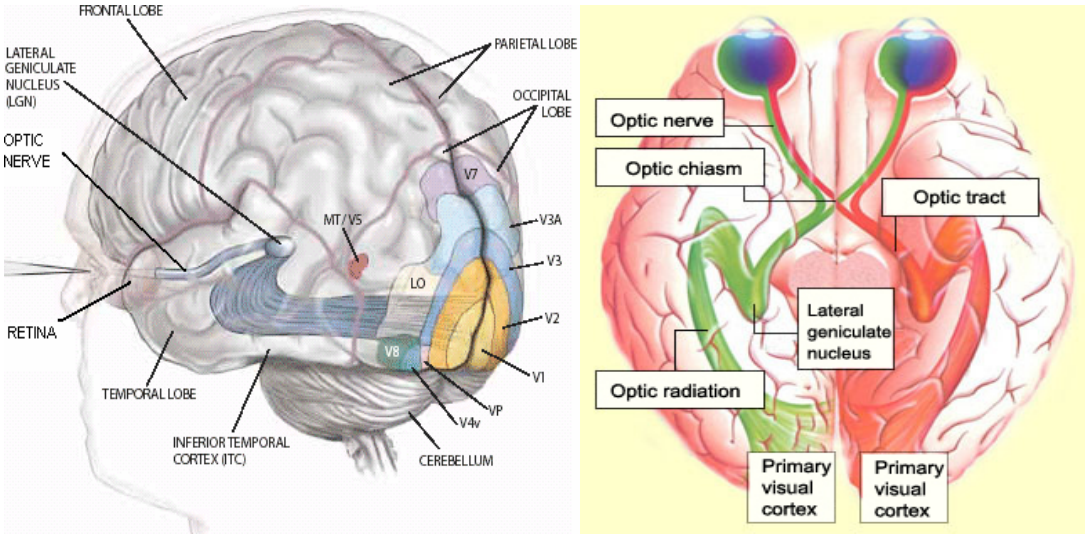

Figure1.1 The primary visual pathway (http://thebrain.mcgill.ca)

1.1.1 The retina

The retina lies at the posterior pole of the eye and is the photosensitive layer where the rays of light are focused on and so the conversion of light energy to electric impulses takes part (see figure 1.2).

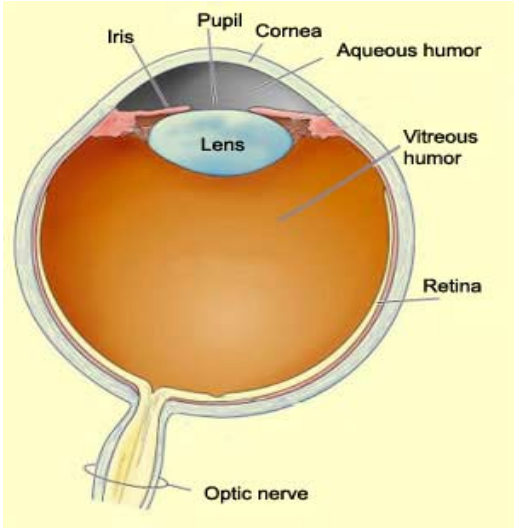

Figure1.2 The eye and the area where the retina lies(http://thebrain.mcgill.ca)

It is about 0.4mm thick (except the area of fovea, which is thinner), about 32mm in length and has three distinctive areas (see figure 1.3):

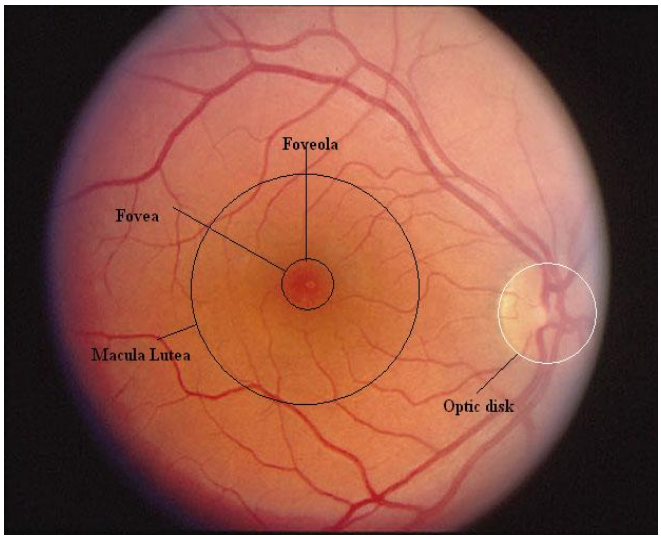

Figure 1.3 The three characteristic areas of the retina

- The macular lutea which is an area of about 5mm ~20° of visual angle,
- The fovea, at the centre of macular lutea with a diameter of about 1.5mm (~5°) and the foveola at the centre of the fovea (~1°). The foveola is the thinnest part of the retina. It approximates to the visual axis and is responsible for high resolution vision because very high density of cones is presented at this point.
- The optic disk which is about 15° of visual angle nasal from foveola.

The retina consists of five different neuron cells, the photoreceptors, the horizontal, the bipolar, the amacrine and the ganglion cells (see figure 1.4). These cells operate to form different paths to the brain.

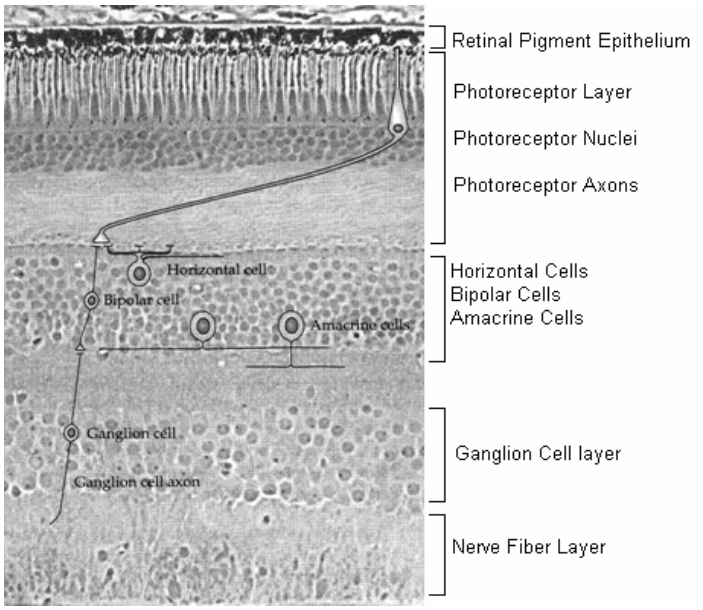

Figure 1.4 The layers of the neuron cells at the retina(Dowling and Boycott 1969)

There are two types of photoreceptors (see figure 1.5), rods and cones. Cones are responsible for colour vision and for vision under photopic and mesopic conditions while rods do not show colour selectivity and are responsible for vision under scotopic conditions. Recently a new type of photoreceptor was found, and said to be responsible for the set of the circadian rhythm(Berson, Dunn et al. 2002). The retina contains about five millions cones and 120 millions rods.

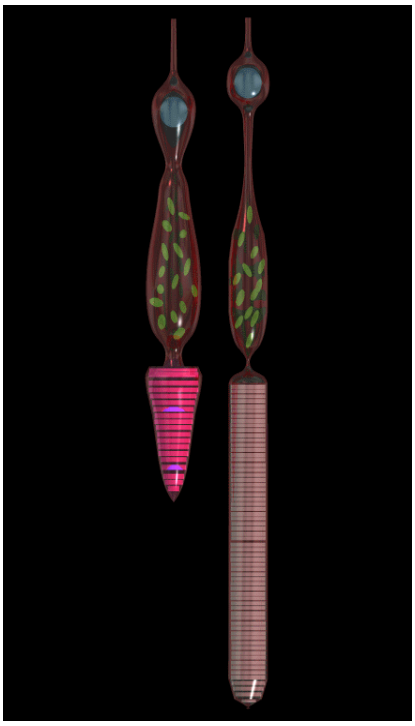

Figure 1.5 Two different types of photoreceptors, cones (left) and rods (right)

The cone density is higher at foveola and decreases to the periphery, rather than the rod density which is higher at about 20° from the centre of macula lutea (see figure 1.6, 1.7).

Rods are absent from the foveola and only cones are present in this area. That is why the foveola has the highest resolution and sensitivity. Also, at the centre of the fovea, each cone is connected to a single horizontal cell but at the periphery more cones and rods converge to different cells.

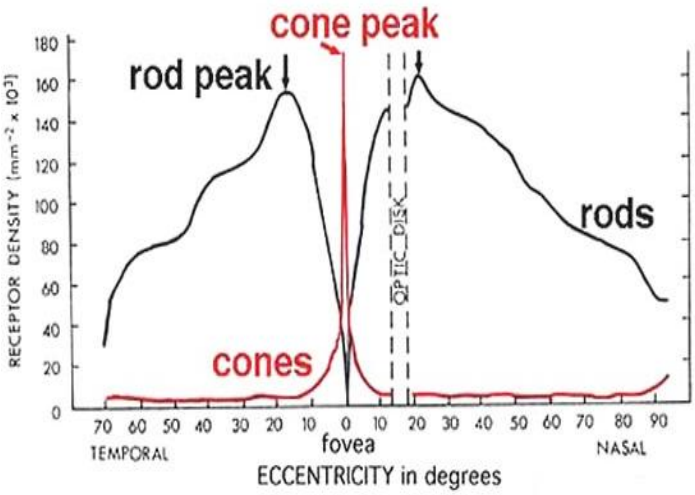

Figure 1.6 The distribution of the photoreceptors density at the retina (http://webvision.med.utah.edu)

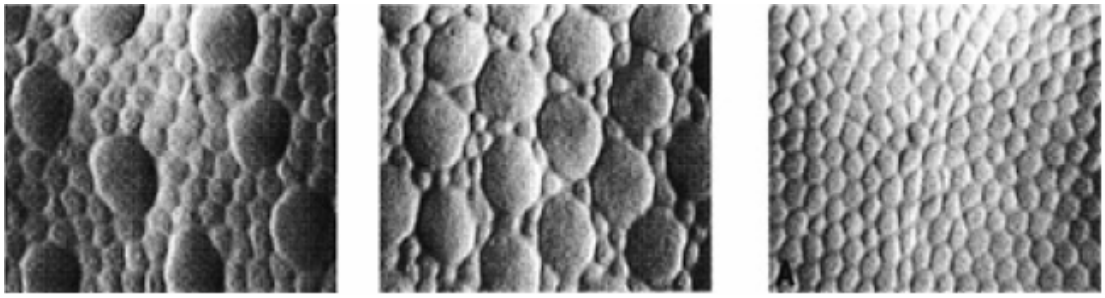

Figure 1.7 The photoreceptors mosaic. Left at 20°, Centre at 5° and Right at the centre of foveola(Curcio, Sloan et al. 1990)

Finally, a reference to the three types of cones must be made. Cones, as already described, are responsible for colour vision. So, there are three types of cones which show different absorption of wavelengths, i.e. the S-cones which are most sensitive at 420nm, the M-cones sensitive at 534nm and the L-cones which are most sensitive at 564nm (see figure 1.8).

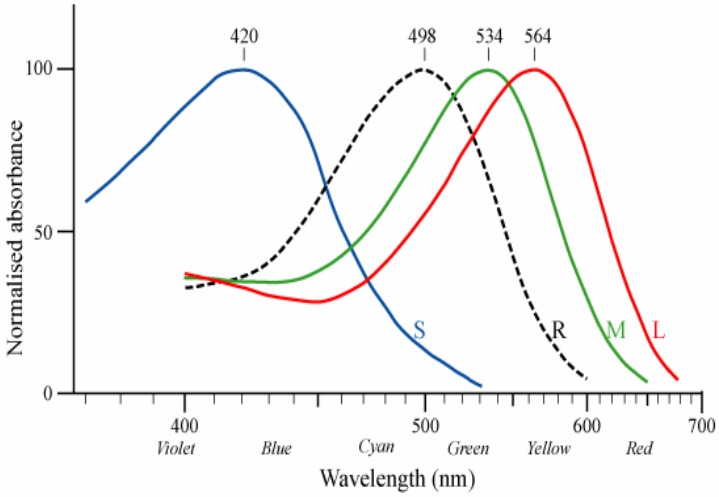

Figure 1.8 The normalized response spectra of human cone S, M, L type and rods(R) (http://wikimedia.org)

The final layer of retinal processing is the ganglion cell layer. The ganglion cells receive signals from a specific area of the retina and always from same photoreceptors. So, any ganglion cell has it own region from which receives an impulse and transmits it to brain. This area is called the receptive field of the ganglion and differs as the retinal area changes. The receptive fields are circular, have two areas, the centre and the periphery, and can be centre ON or centre OFF receptive fields. The centre ON receptive fields respond

when the centre area is lighted and the periphery is not and the centre OFF receptive fields respond only when the centre is not lighted and the periphery is (see figure 1.9).

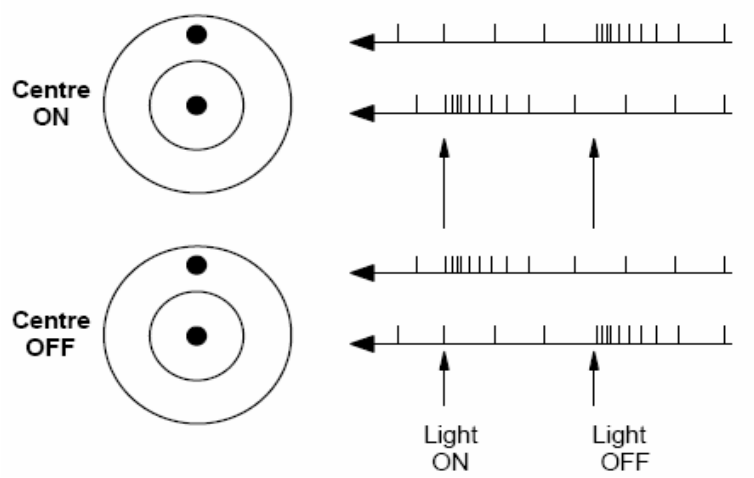

Figure 1.9 The centre ON and Centre OFF receptive fields (RF) with their responses. When the light is on the centre responds at the Centre ON RF and the periphery at Centre OFF RF. Reversely, when the light is off the periphery at the centre ON RF responds and the centre at the Centre OFF RF.

There are also three different types of ganglion cells, the parvo, the magno and the small bistratified ganglion cells and this discrimination has to do with the LGN area to which they project. The parvo cells are the majority of the ganglion cells, have small receptive fields which lie at fovea. Are responsible for colour vision and receive information from the L and M cones (green-red pathway) and project to the P laminae. The magno ganglion cells are fewer than the parvo, have larger receptive fields and receive responses mainly from the periphery of the retina and project to the M laminae. The small bistratified ganglion cells are responsible for the blue-yellow pathway (S cones) and project to the koniocellular laminae.

1.1.2 The Lateral Geniculate Nucleous

As stated in the previous section, the ganglion cell axons consist the optic nerve which exits the eye and terminates in the Lateral Geniculate Nucleous (LGN). There are two LGN, one at each side of the brain and are located in the thalamus. Each LGN is composed of six cellular layers which can be discriminated to two different types (see figure 1.10). The two ventral layers

are the magnocellular and receive data from the magno cells. The four dorsal layers are the parvocellular and receive information from the parvo cells. Each layer receives independent impulses from each eye, so the layers 1, 4 and 6 receive information from the contralateral eye and the layers 2, 3 and 5 from the ipsilateral. Between each layer, the koniocellular layers were recently discovered and they are said to receive inputs from the small bistratified cells(Kaas, Huerta et al. 1978)

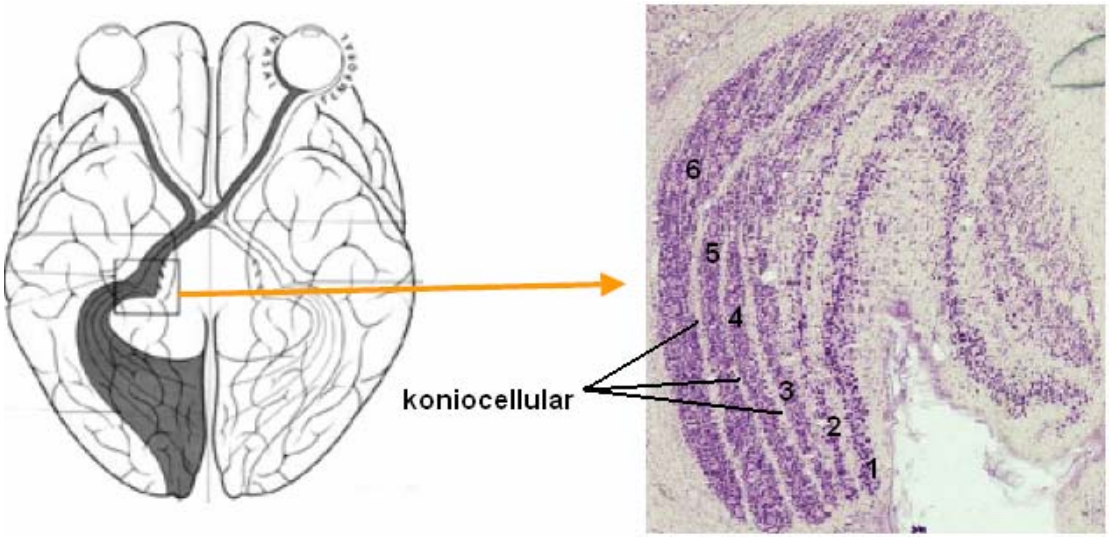

Figure 1.10 The LGN. 1 and 2 layers are connected with the Magno cells, 3, 4, 5 and 6 with the Parvo cells and the koniocellular layers with the small bistratified cells. Also, at this specific diagram, layers 1, 4 and 6 receive information from the right eye (contralateral) and the 2, 3 and 5 from the left eye (ipsilateral) (http://phineasgage.wordpress.com)

As each layer receives information from a specific area of the retina it can be suggested that the layers are a retinotopic map and represent a single area of the visual field. Also, the parvocellular layers receive impulses only from the centre area of the retina (proximal 5^{o}) but are represented in over half of the LGN.

1.1.3 The primary visual cortex

After the LGN the process of the input signal takes part at the Primary Visual Cortex where the majority of the fibres from the LGN terminate via

the white matter of the brain. The Primary Visual Cortex, which is also called striate Visual Cortex or V1, lies in the occipital lobe at the rear part of the brain. V1 which consists of six layers of cells, is about 1.5mm thick and has a striated appearance (that is why it is called Striate Visual cortex). The Parvo cells axons from the LGN terminate at the lamina $4C_{\beta}$ and 4A while the Magno cells axons terminate at the $4C_{\alpha}$ laminae (see figure 1.11). Afterwards, the received information terminates at the other layers of V1. From $4C_{\alpha}$ to 4B, from $4C_{\beta}$ to layers 2, 3 and finally to other areas of the cortex and to deeper structures of the brain.

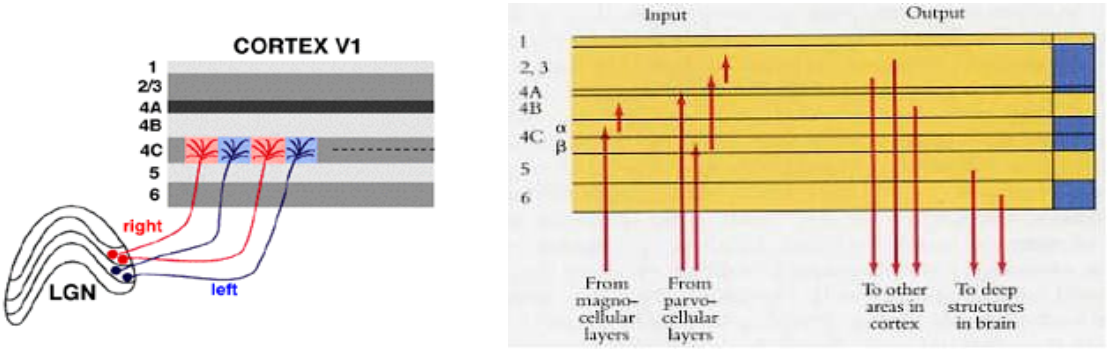

Figure 1.11 The Parvo and Magno cells from the LGN send information at the 4C and 4A layer at V1(left)(http://webvision.med.utah.edu). From the 4C layer, further processing takes part at the other layers of V1 and finally to other structures of the brain (right)(http://hubel.med.harvard.edu)

The V1 has two types of cells, the simple and the complex cells. The simple cells have inhibitory and excitatory regions, are elongated and show orientation selectivity. The excitatory and inhibitory domains are always separated by a straight line or by two parallel lines and also the two regions show antagonism. The complex cells, which are more numerous than the simple, show orientation selectivity, do not have excitatory or inhibitory regions and appear to have directional selectivity which mean that respond better when the stimulus moves to one certain direction(Hubel 1988)(see figure 1.12, 1.13)

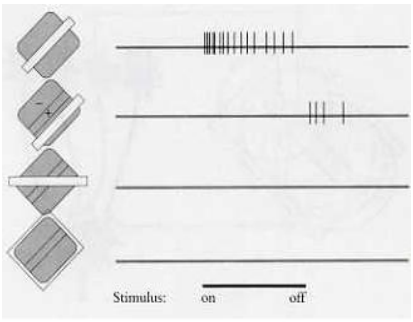

Figure 1.12 The responses of a simple cell. Top: The response to a bar of optimum size, position and orientation. Second: While the same bar cover a field of the inhibitory area. Third: Different orientation than the optimum. Bottom: The whole receptive field is illuminated. (http://hubel.med.harvard.edu)

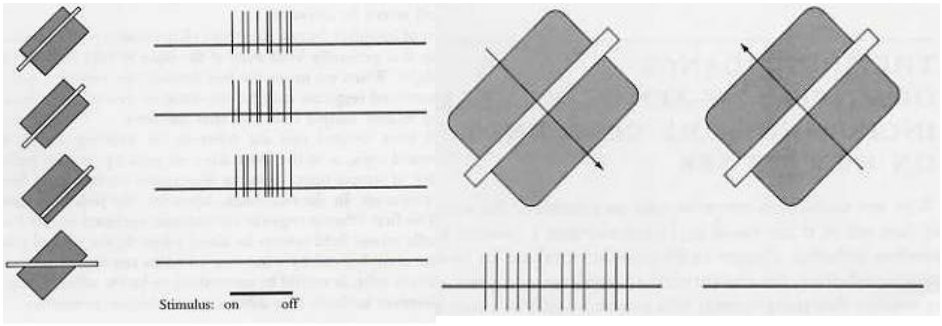

Figure 1.13 The responses of a complex cell. A long, narrow bar of light produces a response wherever it is placed (left). The responses also differ with the movement direction of the bar(right).(http://hubel.med.harvard.edu)

The cortical cells are much more selective for stimulus width than the ganglion cells. Cortical cells with small receptive field response at high spatial frequencies while those with large receptive fields at low spatial frequencies(Hubel 1988).

In layer 4C at V1, the cells appear to be driven monocularly. Thus, there is a structure of regions which are stimulated by left or right eye. These regions are called ocular dominance columns and appear to be more complex away from the input layer of V1. These columns are about 0.5-0.6mm thick and lie across the cortical surface. There are some models for the structure of V1 as is the "ice cube model" which shows that the cortex is divided into two kinds of slabs, one for ocular dominance and the other for orientation(see figure 1.14)(Hubel 1988). Within these columns there are different orientation selective receptive fields and consequently all possible combinations of orientation and ocular dominancy are present (Hubel 1988).

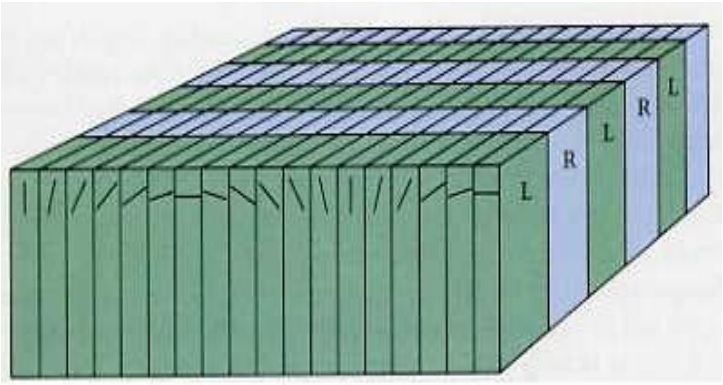

Figure 1.14 The ice cube model suggested by Hubel. There are two dimensional columns, for ocular dominancy at one direction and for orientation selectivity at the other(Hubel 1988).

Electrophysiological studies found that the cortical cells show selectivity at spatial frequency. A number of cells which are selective at the same spatial frequency is said to consist a spatial selective neural channel (Campbell, Cooper et al. 1969; Webster and De Valois 1985; Tootell, Silverman et al. 1988) (see figure 1.15) Many models have been introduced at which there are no edges between the areas and others where the columns are three dimensional while at the third dimension there is the spatial frequency

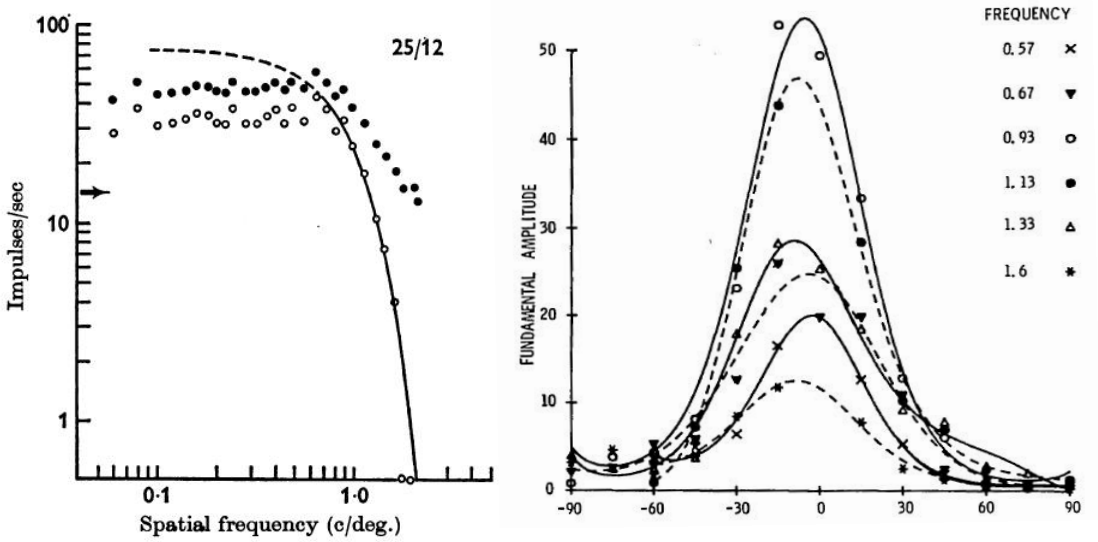

Figure 1.15 Electrophysiological evidences of spatial frequency selectivity at cortical cells. Grater responses rates (left(Campbell, Cooper et al. 1969)) and response amplitude (right(Webster and De Valois 1985)) of the striate cells at a certain spatial frequency.

At last, we have to refer to the phenomenon which called cortical magnification. The retinal areas with high visual resolution (i.e. fovea) are represented in a bigger area at V1, while the areas with low resolution (i.e. periphery) project to a small area. This has to do with the fact that the central vision carries the huge amount of useful visual information (see figure 1.16).

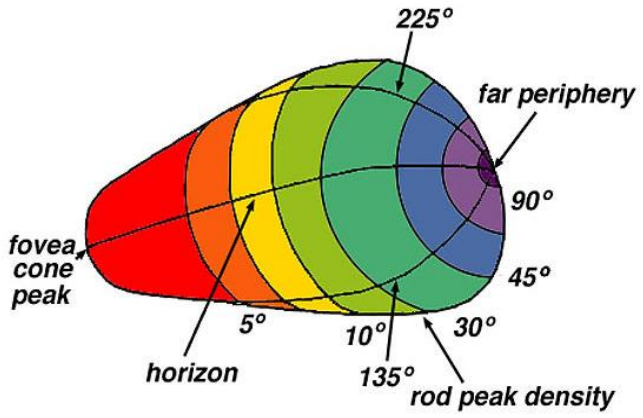

Figure 1.16 The pear shaped striate cortex. The far periphery is much underrepresented that the half circle corresponding to 90° is very small (http://webvision.med.utah.edu)

The major part of V1s outputs project to V2 which is responsible for stereopsis and object direction. V2 sends its outputs to V3, V4 (where the colour and form are said to be analysed) and MT/V5 (medial temporal) where the depth and motion of the objects are analysed. These areas, at the next step of the process, send information at superior colliculus, higher visual areas (V7, V8), posterior parietal core which is responsible for space perception, and various subdivisions of the thalamous. Also, each of these areas project back to the area or areas from which it receives input.

1.2 Psychophysics

Neurophysiologists and anatomists explore the brain from inside, trying to find where different cell axons terminate, recording responses of the cells during the presence of a stimulus, using techniques to image the different functional areas. Another scientific area was developed, to understand how and why neuron cells respond to certain visual stimulus and how the visual

processes occur, using non invasive techniques, and is called psychophysics (from the Greek psycho=soul and Latin physica=nature). This area tries to correlate a stimulus or/and a certain trial with a subjects perception and respond(definition: psychophysics is a sub discipline of psychology dealing with the relationship between physical stimuli and their subjective correlates, or percepts(http://wikimedia.org)). It considers the brain as a black box and search to find a relation between the input and the output of the sensory system (see figure 1.17).

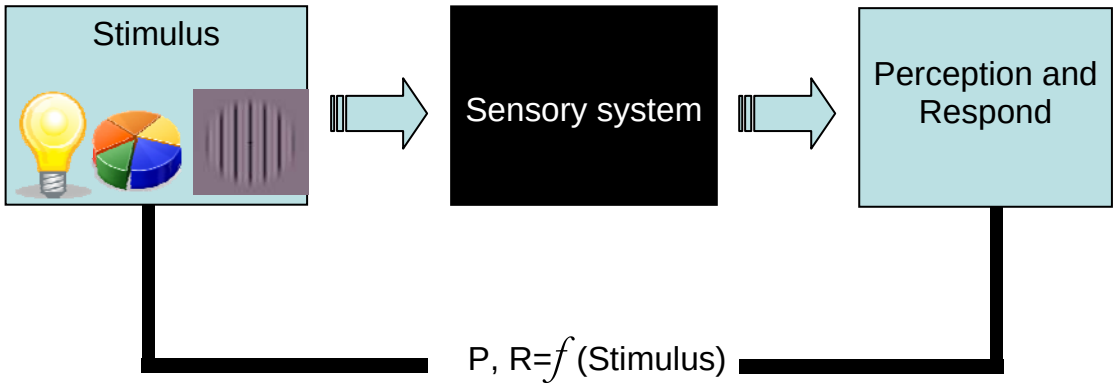

Figure 1.17 Psychophysics correlates with a function the output and the input of the sensory system.

Many psychophysical methods have been used to establish normal levels of vision and the range of these values in people with normal vision. Psychophysical measurements can also be used analytically to test hypothesis about the neural mechanisms that underlie the perceptual response of the subject.

There are many different psychophysical methods that give accurate, reliable results with the fewest number of stimulus presentations, without requiring sophisticated judgements on the part of the patient and with minimal opportunities for psychophysical bias to affect the results(Norton, Corliss et al. 2002). Most of them are designed so that the subject sets his threshold for a definite stimulus. Threshold is the minimum amount of a stimulus required to detect the presence of that stimulus under ideal

conditions. So, the sensitivity for this stimulus can be calculated and is the reciprocal of the threshold. The most common methods to determine the threshold are the:

- Method of Adjustment in which the subject can adjust a variable of the stimulus to find the minimum value of this variable at which the stimulus is still present.
- Method of Limits in which a value sequence of the variable is presented in a descending or an increasing way until the subject detects the stimulus.
- Method of Constant Stimuli in which a sequence of pre-adjusted values of variables is presented to the subject which has to respond either yes when sees the stimulus nor no when the stimulus is not visible. For the determination of the threshold, a graph has to be made (see figure 1.18)

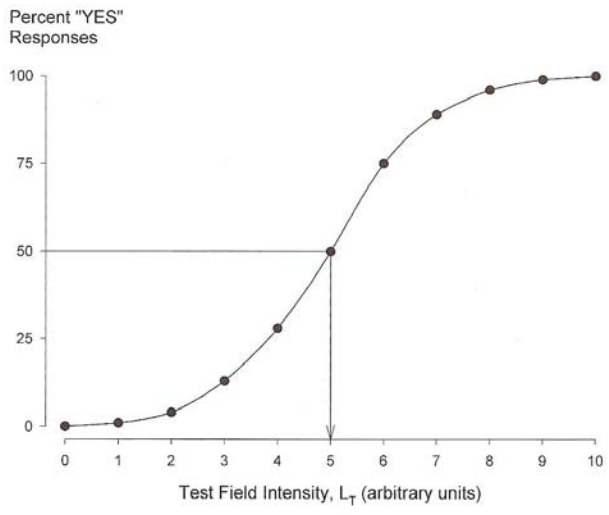

Figure 1.18 The graph for the determination of the threshold with the method of constant stimuli (graph is known as the psychometric function). At the y axis there is the percent 'yes' responses and at the x axis the values of the variable. The threshold is usually set at the 50% of the affirmative answers(Norton, Corliss et al. 2002).

- The forced choice procedure in which some stimulus are presented with different variables either with temporal difference or spatial difference and the subject s forced to choose one of the time intervals or one of the positions in which he thought the stimulus appeared.

- The adaptive method which is an up-to-date version of the method of the method of limits which uses some algorithms to find the threshold.

There are definitely some reasons because of which the values of threshold vary. One reason is the random fluctuations in the stimulus occuring during the experiment which can impact the threshold measurements. Another reason is the physiological fluctuations in the activity levels (noise) of the neurons. The attention and the alertness of each subject are further reasons due to which the threshold measurements vary and finally the psychological bias and the proper criteria of the subjects are enough to change these values.

Psychophysical experiments take part in the daily routine of the optometrists and the ophthalmologists. The most common is the visual acuity test with letter charts in which the subject/patient has to recognize the smallest letter so that the examiner calculates his visual acuity. Other tests are the visual reaction time test where the subject has to respond (usually by pressing a button) when perceives a certain stimulus. Also, some psychophysical tests have been designed to examine the colour visual performance (i.e. colour matching).

The visual system is developed in a manner to recognize and detect objects by the difference in luminance at their edges and this is associated with the receptive fields at the retina and consequently at the striate visual cortex as cited at previous sections. Thus, needs studying this attribute force to figure a psychophysical experiment for the spatial visual performance.

1.2.1 Spatial contrast sensitivity.

To correlate the natural scenes with the anatomic-physiological brain characteristics and the neuron responses was necessary to develop a trial which simulate the scenes of the surrounding environment. Such a psychophysical experiment is the spatial contrast sensitivity which developed in mid sixties. During this experiment, several stimuli are projected and the subject is asked to find the contrast threshold (C_{min}), the reciprocal of which is the contrast sensitivity (CS):

$$CS = \frac{1}{C_{\min}}$$

Given that the visual system responds well to spatial changes in luminance, an obvious way to characterize the ability of the visual system to detect such changes is to measure the threshold contrast needed to see spatially varying stimuli. So, sine wave gratings are projected to a high resolution monitor in different spatial frequencies and contrast. The luminance profile (see figure 1.19, 1.20) of such a grating can be described with the mathematical expression:

$$L(x) = L_m[1 + c\sin(2\pi Fx + \varphi)]$$

where L(χ) is the luminance at position χ, L_m is the mean luminance $L_m = \frac{L_{\max} + L_{\min}}{2}$, c is the Michelson contrast $c = \frac{L_{\max} - L_{\min}}{L_{\max} + L_{\min}}$, L_{max} and L_{min} the maximum and the minimum luminance respectively, F the spatial frequency in cycles per units of χ, χ is the horizontal position and φ is the spatial phase.

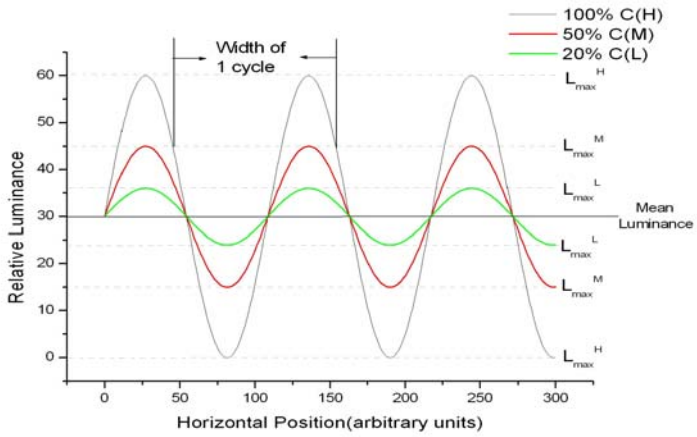

Figure 1.19 Relative luminance profiles for 100% contrast (H), 50% (M), 20% (L) sine wave gratings

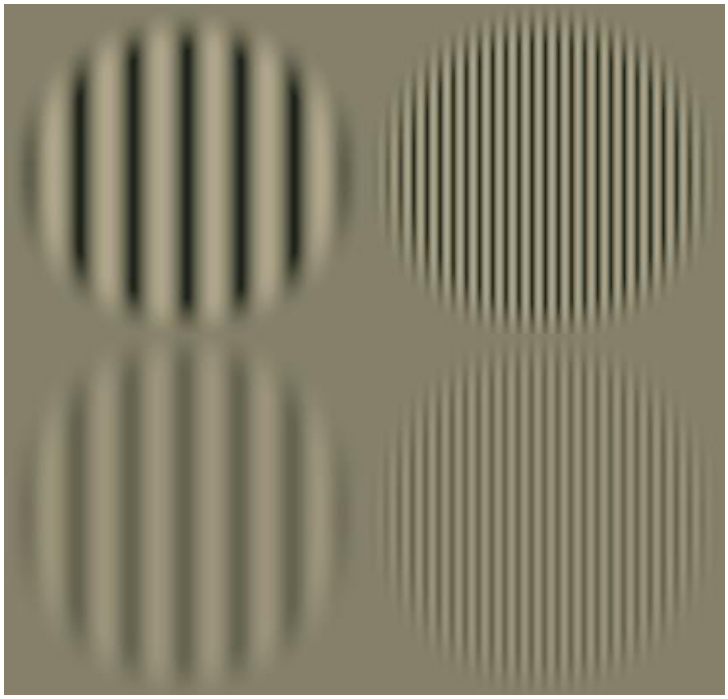

Figure 1.20 Top: Vertical orientated gratings of low (left) and high (right) spatial frequency at 100% contrast as they projected to a monitor. Bottom: Same gratings as above but at 50% contrast.

Using gratings as in figure 1.20 at a range of spatial frequencies and many different contrasts, the threshold contrast for each spatial frequency can be found and the contrast sensitivity can be calculated. Plotting the contrast sensitivity as a function of spatial frequency the contrast sensitivity function can be obtained which gives many useful information (see figure 1.21)

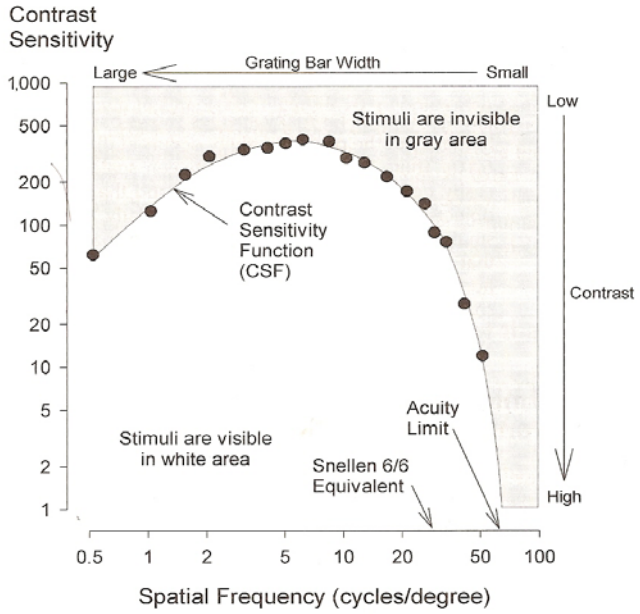

Figure 1.21 A typical contrast sensitivity function (see text for details)(Norton, Corliss et al. 2002)

The contrast sensitivity function (CSF) has generally an inverted U-shape and the areas below and above the line represent the areas where the gratings are visible (below) and invisible (above). From this function the peak contrast sensitivity can be found and for the certain CSF is approximately 6cycles per degree. For humans the peak contrast sensitivity lays between 3 to 10 c/degree depending on the conditions. It is obvious that only a select range of spatial frequencies is detected and this means that the visual system works as a band pass filter. The gradual decrease in sensitivity at low spatial frequencies is called the low spatial frequency roll-off while the highest spatial frequency that can be detected at maximum contrast is called the cut-off high spatial frequency and occurs between 30 to 60c/degree and this because the 60c/degree is the maximum spatial frequency which can be resolved by the human visual system (nycuist limit). If someone has 1arcmin resolution acuity then the cutoff frequency should be at approximately 30c/degree (see the Snellen 6/6 equivalent at figure 1.21). The contrast sensitivity function is affected by defocus which blurs the image on the retina with a resulting reduced. For low spatial frequencies

defocus does not have a big effect on the contrast because the light and dark bars are not close enough to each other but at high spatial frequencies where the bars are more densely spaced defocus reduces the contrast below threshold (see figure 1.22)(Campbell and Green 1965). Also, defocus can be produces by cataract and other conditions affecting the optics of the eye.

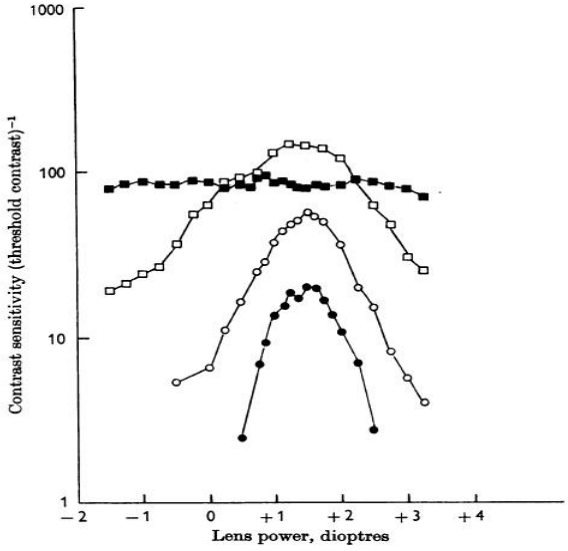

Figure 1.22 The effect on contrast sensitivity of changing the refractive power of the eye. The points are the average of three measurements. Black circles: 30 c/deg; open circles: 22 c/deg; open squares: 9 c/deg; black squares: l.5 c/deg.(Campbell and Green 1965)

The CSF varies with illuminance in three ways: 1) The peak contrast sensitivity shifts toward lower spatial frequencies as the illuminance decreases, 2) the cutoff high spatial frequency occurs at a lower spatial frequency with lower mean retinal illuminance and 3) the low spatial frequency rolloff becomes less observable as the retinal illuminance falls, until it completely disappears. The first two reasons can easily be explained by the passage from photopic cone-driven receptive fields (small→high spatial frequency) to scotopic rod-driven receptive fields (large→low spatial frequency). The retinal eccentricity is another factor which changes the CSF. Because the receptive fields, which determine the peak spatial contrast sensitivity and the cutoff high spatial frequency, become larger with distance from the fovea the CSF is shifted toward lower spatial frequencies as a function of increased retinal eccentricity. Another reason is the convergence of many photoreceptors to one ganglion cell which is more pronounced at eccentric retinal location (see figure 1.23).

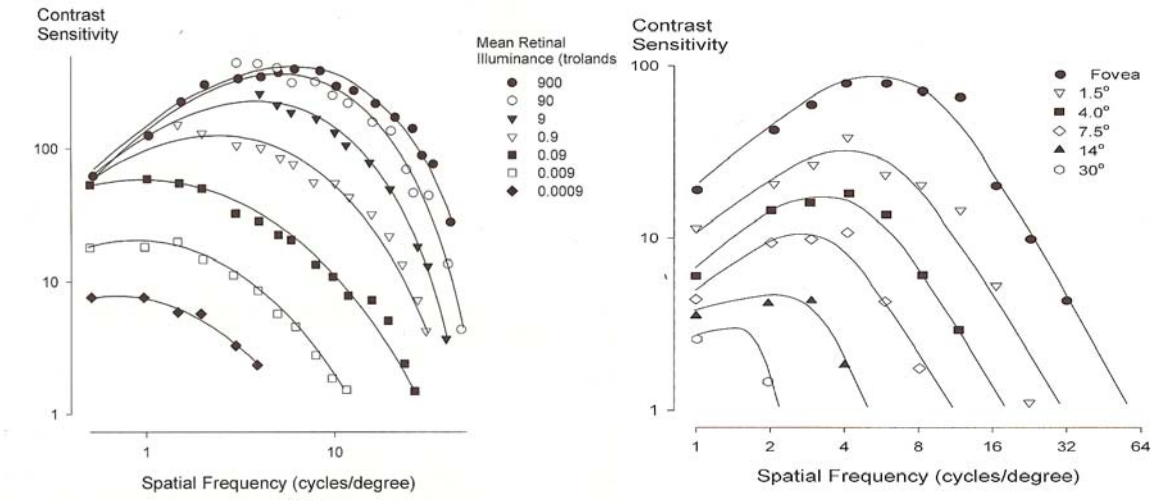

Figure 1.23 The changes at human CSF as a function with retinal illuminance (left) and retinal eccentricity (right). The amount of spatial information that can be processed by the visual system decreases with decreasing retinal illuminance and increasing retinal eccentricity(Norton, Corliss et al. 2002).

As referred in previous pages, even though the ganglion receptive fields are circular at striate visual cortex the receptive fields are prolate and for that reason are tuned to orientated stimuli. As a result, the contrast sensitivity changes with the orientation with the maximum at 90º and 180º degrees (see figure 1.24)

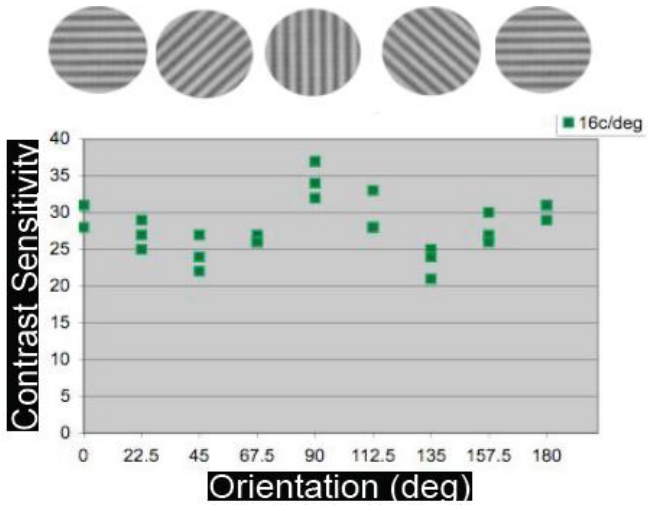

Figure 1.24 The contrast sensitivity depends on orientation of the gratings and presents higher while is at horizontal or vertical orientation (for high spatial frequencies i.e. 16c/deg)(Plainis)

Also, the CSF shifts towards lower contrast sensitivity and lower cutoff high spatial frequency as the eye ages. For this fact there are anatomical, physiological and psychophysical evidences that there are age related changes in the magnocellular pathway, the rod signals pass through ganglion

cells that project to both the parvocellular and magnocellular layers of the lateral geniculate nucleus (LGN)(see figure 1.25)(Schefrin, Tregear et al. 1999).

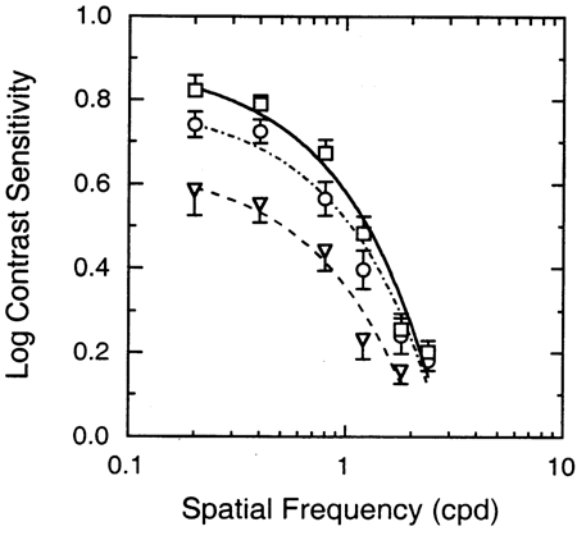

Figure 1.25 Contrast sensitivity for three age groups plotted. The squares, circles, and triangles represent sensitivities for subjects aged 20–40, 41–60, and 61–88 years, respectively(Schefrin, Tregear et al. 1999).

Diseases which affect the optic elements of the eye and the neuronal system affect also the contrast sensitivity. Such diseases are cataract, glaucoma, keratoconus and amblyopia. Most of these conditions depress the contrast sensitivity at high spatial frequencies, so that these conditions are also detected by simple measures of the visual acuity.

1.2.2 Individual neurons with a spatial contrast sensitivity function

As cited above, the CSF determined psychophysically measures the contrast sensitivity of the visual system as a whole. But, the performance of the visual system depends on the responses of individual neurons in the retina, the LGN and striate cortex(Norton, Corliss et al. 2002). The contrast sensitivity function has been measured in a variety of species by electrophysiologically recording the activity of single cells in different layers at the visual pathway and found that individual retinal and LGN cells have spatial CSFs that superficially resemble the spatial CSf of the whole visual system. Each of these cells shows a low frequency roll-off, a cut-off high

spatial frequency and peak contrast sensitivity and these are reasons from which can be assumed that each cell operates as a band pass filter. The neuron cells in V1 found to be narrowly more band pass than does the entire visual system. It can be concluded that the spatial CSF is composed of the spatial CSFs of a variety of neurons each providing contrast sensitivity to a different narrow band of spatial frequencies (see figure 1.26). The fact that a retinal ganglion cell has a band pass spatial CSF can be explained considering the receptive fields and their responses to sine wave gratings of different spatial frequencies. Each cell responds stronger when its centre and its surround is lighted or not with a light/dark bar of such a width which mach the width of the centre and the surround, depending if it is centre-on or centre-off (see figure 1.27).

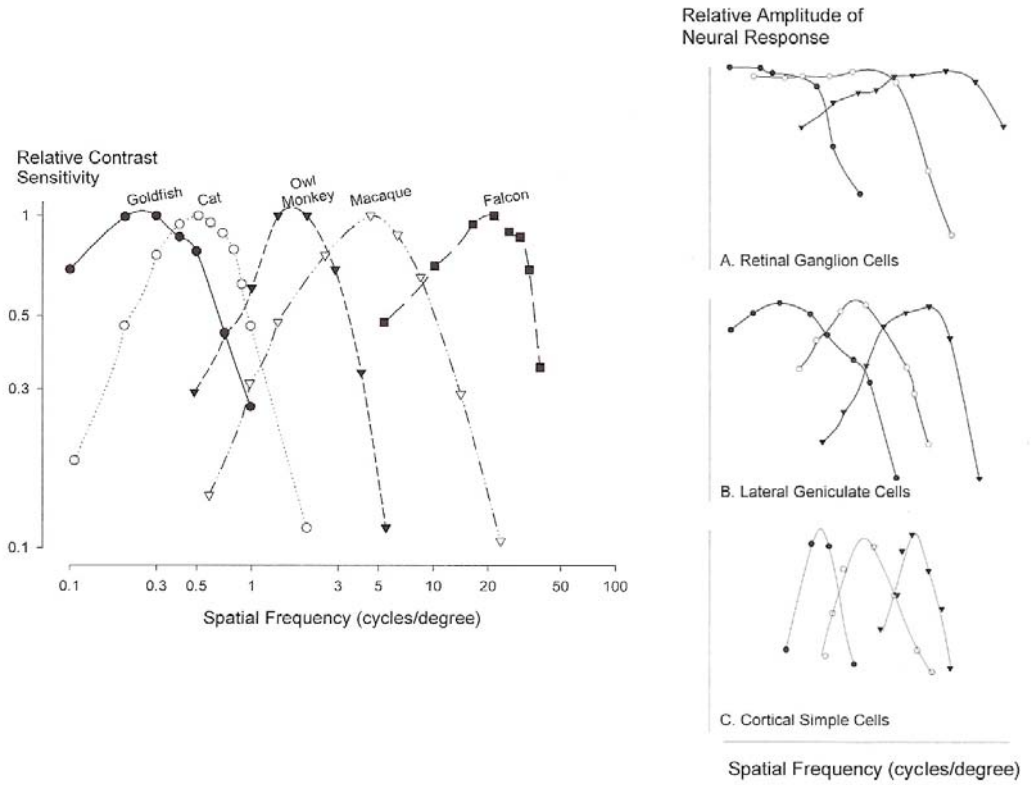

Figure 1.26 The CSFs measured psychophysically for 5 species (left) and cats' cell responses at different parts of the visual pathway (right). It's obvious that the CSFs of retinal ganglion cells and laterals' geniculate nucleus cells differ a lot from the overall CSF(Norton, Corliss et al. 2002).

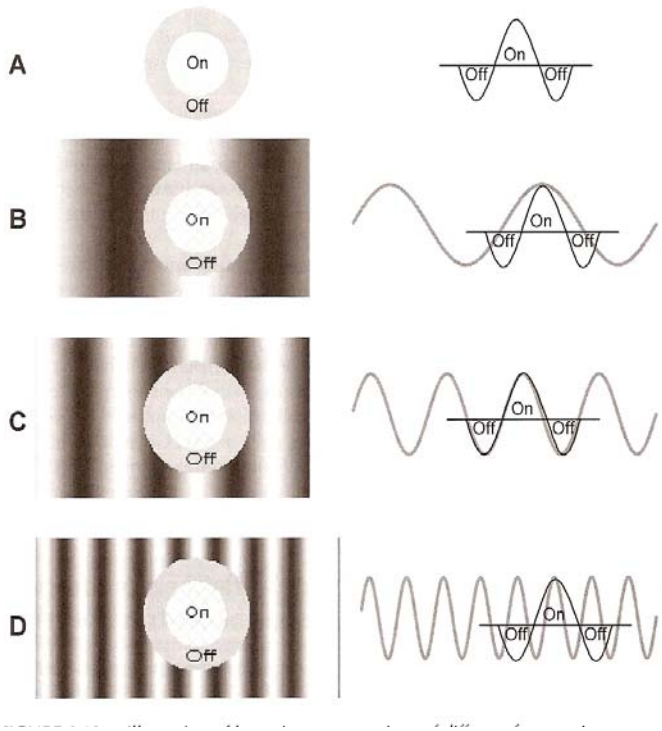

Figure 1.27 A centre-on receptive field superimposed to different spatial frequencies. The cell responds strongest at case C where the whole centre is exactly lighted and the whole surround is not. The other two cases produce week responses due to the phenomenon of lateral inhibition(Norton, Corliss et al. 2002).

Figure 1.27 suggests that centre-surround cells are generally band pass. Cells with smaller centres have peak contrast sensitivity at a higher spatial frequency while those with larger centres have peak contrast sensitivity at lower spatial frequencies. As discussed in neurophysiology, in primates, cells with smaller receptive fields tend to be part of a parallel pathway from the retina to the cortex (the parvocellular pathway) and seem to be responsible to the detection of high spatial frequencies and discretion of colour, while cells with larger receptive fields tend to be a part of the magnocellular pathway and appear to be responsible for the ability to detect low spatial frequency stimuli particularly when they are moving or flickering.

1.2.3 Multiple spatial frequency channels in the visual system

Before advanced single cell electrophysiological techniques were developed, Campbell and Robson first reported that the visual system may consist of many narrowly tuned spatial frequency channels. They came to this conclusion because they found that for spatial frequencies over a certain

value the sine-wave gratings have approximately ($\pi/4$ less for being accurate) the same contrast sensitivity with the first harmonic of square wave gratings at same contrast but for spatial frequencies lower than a certain value the sine-wave gratings have smaller contrast sensitivity than the square wave gratings. Thus, they supposed that the visual system behaves not as a single detector mechanism preceded by a single broad-band spatial filter but as a number of independent detector mechanisms each preceded by a relatively narrow band filter tuned to a different frequency(Campbell 1968).

Later, Blakemore and Campbell run some psychophysical experiments and showed that individual spatial frequency channels exist in the human visual system(Blakemore and Campbell 1969). They first measured the spatial contrast sensitivity using common psychophysical methods. After, having adapted the subjects to gratings of high contrast of a certain spatial frequency they measured the contrast sensitivity again. At this experiment the subject was exposed to a high contrast grating of 7.1c/degree. Their hypothesis was that if the visual system is mediated by a single detector, then the adaptation should affect the whole spatial contrast sensitivity function but if it is consisted of many narrowly tuned spatial frequency channels then the adaptation should affect only the particular spatial frequency and a small range around this frequency. They found that the exposure to a high contrast grating of a particular spatial frequency temporarily raises the threshold for detecting that grating, which means that the contrast sensitivity is depressed (see figure 1.28).

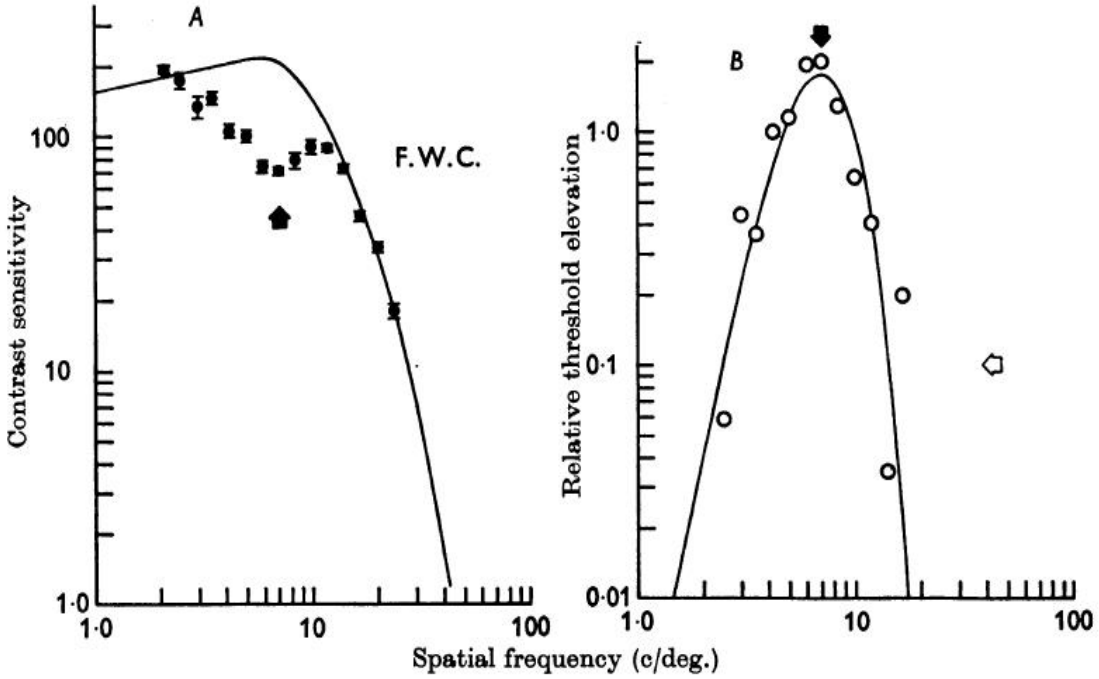

Figure 1.28 The contrast sensitivity function without adapting the observer to a high contrast spatial frequency (straight line) and after adaptation at 7.1c/degree high contrast grating (black circles)(left graph). The difference between the common and the after-adaptation contrast sensitivity (right)(Blakemore and Campbell 1969)

Blakemore and Campbell reproduced this experiment for different spatial frequencies (see figure 1.29) and came to the conclusions that:

- there is a temporary fivefold rise in contrast threshold after exposure to a high contrast grating of the same orientation and spatial frequency,
- by determining the rise of threshold over a range of spatial frequency for a number of adapting frequencies it was found that the threshold elevation is limited to a spectrum of frequencies with a bandwidth of just over an octave at half amplitude, centred on the adapting frequency,
- the amplitude of the effect and its bandwidth are very similar for adapting spatial frequencies between 3 c/deg. and 14 c/deg. At higher frequencies the bandwidth is slightly narrower. For lower adapting frequencies the peak of the effect stays at 3 c/deg

- these and other findings suggest that the human visual system may possess neurones selectively sensitive to spatial frequency and size. The orientational selectivity and the interocular transfer of the adaptation effect implicate the visual cortex as the site of these neurones.

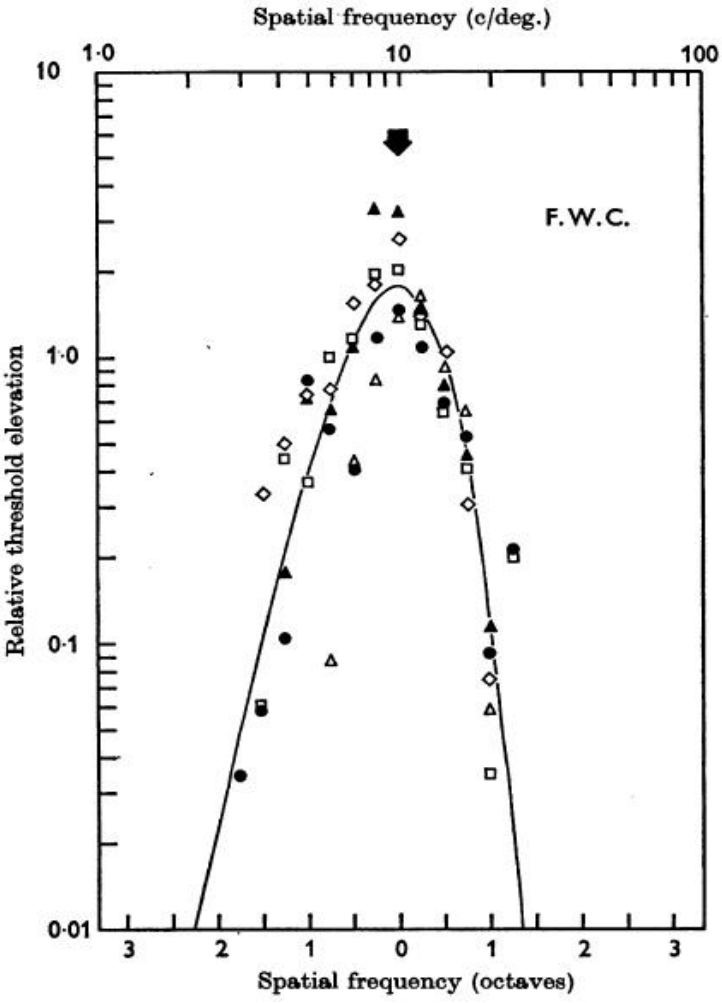

Figure 1.29
The threshold contrast elevation after adaptation to different spatial frequencies (filled triangles:3,5c/deg, filled circles:5c/deg, open squares:7.1c/deg, open rectangular :10c/deg, open circles:14.2c/deg). Blakemore and Campbell found that these data fit best to function $[e^{-f^2} - e^{-(2f)^2}]^2$ and that the full width at half maximum is about 1.3 octaves(Blakemore and Campbell 1969).

So, there are psychophysical, physiological and anatomical evidence supporting the suggestion that the spatial CSF represents the envelope of more narrowly tuned spatial frequency channels. The generalized notion of a channel refers to a filtering mechanism which passes some, but not all, of the information that may impinge upon it, each specialized in a narrow spectra of spatial frequencies with FWHM (Full Width at Half Maximum) about one octave (see figure 1.30).

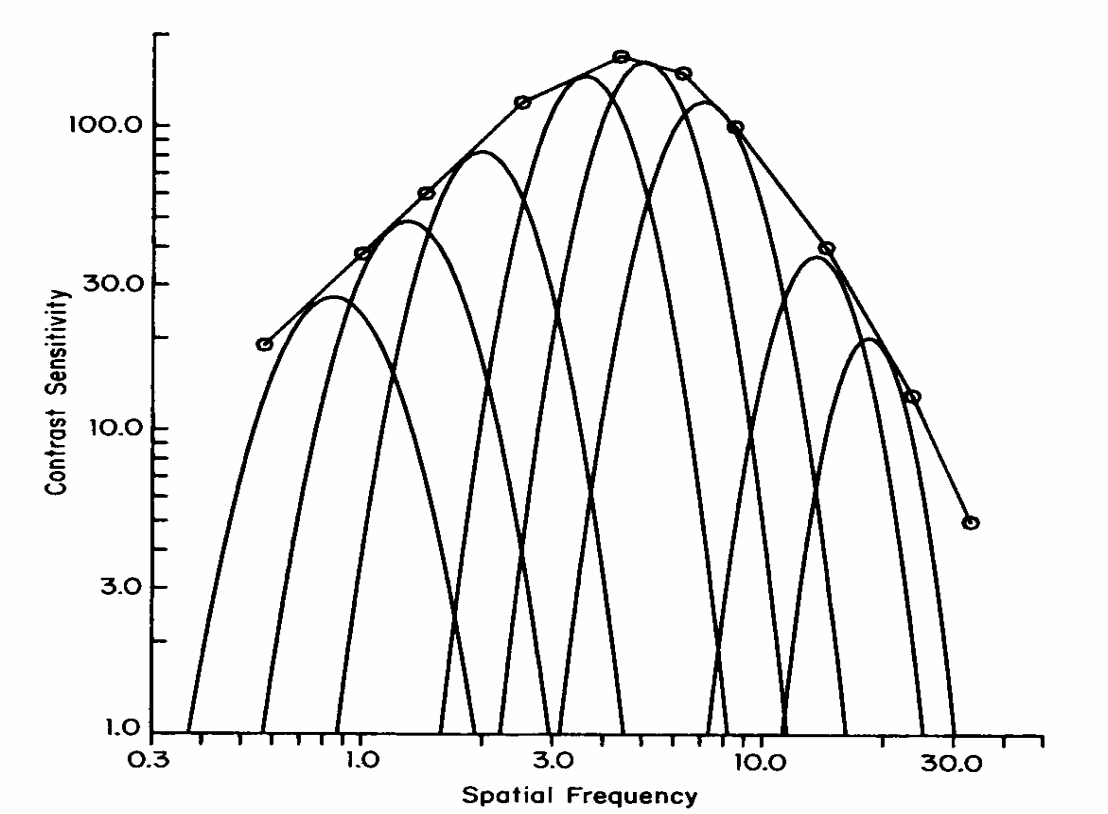

Figure 1.30 The contrast sensitivity function of the whole system as en envelope of the contrast sensitivities of the spatial frequency channels(DeValois and DeValois 1990).

Since then many efforts were made to calculate how many channels there are at a given retinal area and find an index of spatial summation which mean how close these channels are. Many works like Watson's(Watson 1982), Graham's(Graham and Nachmias 1971; Graham and Robson 1987), Limb's(Limb and Rubinstein 1977), Quick(Quick, Mullins et al. 1978) and others estimated the bandwidth of these channels using a large range of spatial frequencies. In order to measure this parameter of the visual system they used gratings composed by two spatial frequencies, so that different channels were been activated.

1.2.4 Compound gratings

To activate two different spatial tuned neuron channels there is a need of using grating composed of two different spatial frequencies. These gratings are called compound gratings and are the sum of two components

sinusoidal gratings each at different spatial frequency, contrast and phase. The mathematical formula that describes these gratings is:

$$L(x) = L_m(1 + c_1 \sin(2\pi F_1 x + \varphi_1) + c_2 \sin(2\pi F_2 x + \varphi_2))$$

where L(χ) is the luminance at position χ, L_m is the mean luminance, c is the Michelson contrast, F the spatial frequency in cycles per units of χ, χ is the horizontal position and φ is the spatial phase. It is possible to add spatial frequencies at every possible spatial and contrast ratio and acquire the luminance profile of a compound grating. The sum of two gratings is represented below and at next graphs there are the luminance profiles of these gratings (see figure 1.31, 1.32, 1.33, 1.34, 1.35).

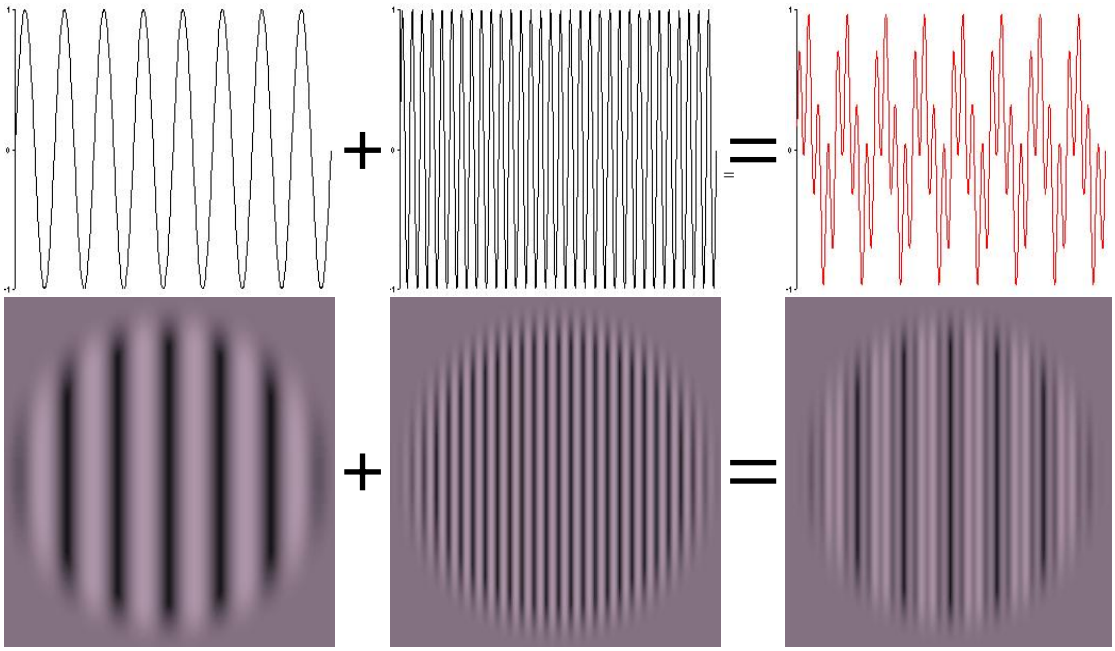

Figure 1.31 The luminance profiles of two single gratings (first and second figure) and their sum (last) (top) and how these gratings are projected to a monitor (bottom).

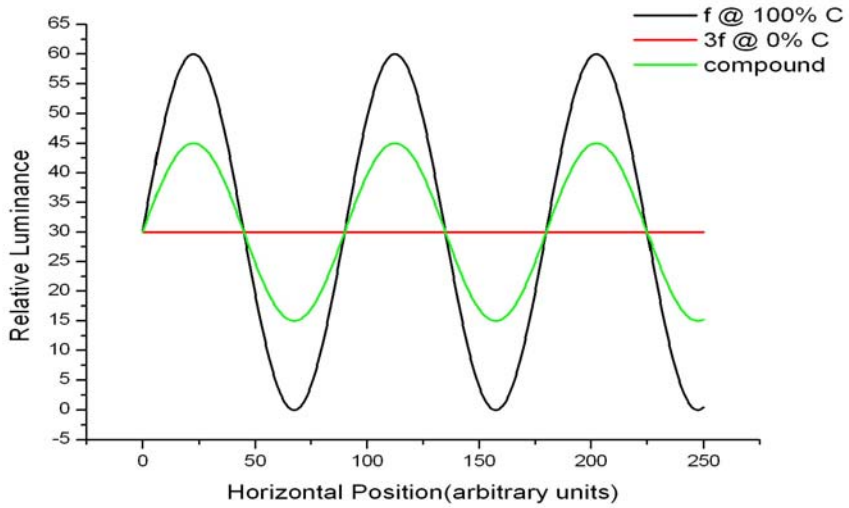

Figure 1.32

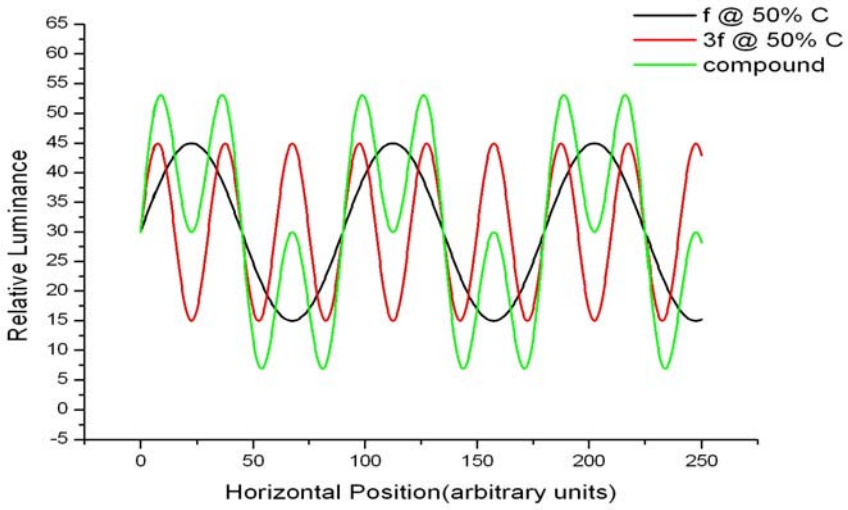

Figure 1.33

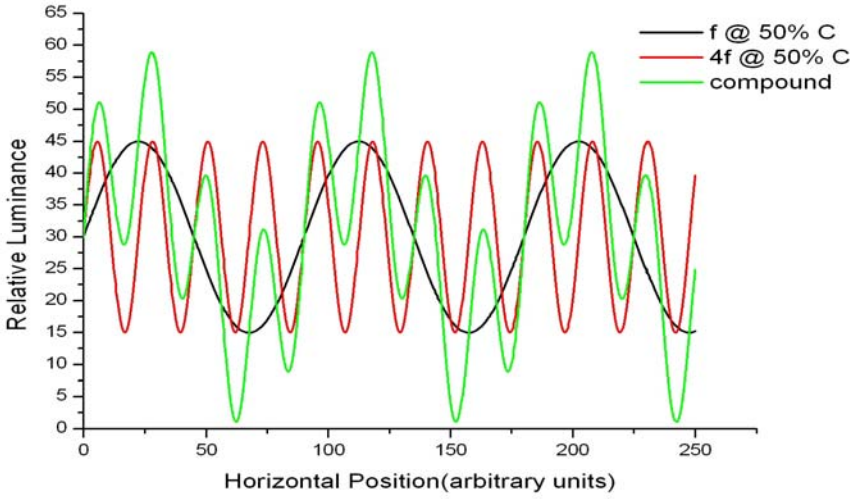

Figure 1.34

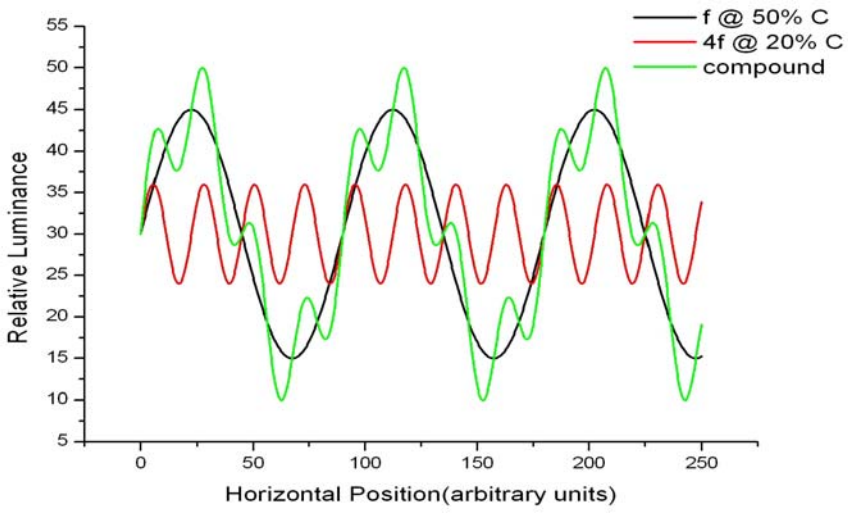

Figure 1.35

From these figures anyone can beware of the elevated contrast of the compound figures because of the different minimum and maximum values of the luminance. This suggests that the compound gratings are much more visible of the single gratings from which they are composed. But, this fact does not happen because of the multiple spatial tuned neuron channels which detect the individual components and not the whole compound grating as a single one. Thus, the compound grating is slightly more visible than the individual gratings, when channels are supposed to be independent, and this happens because of probability summation.

If during a trial where the two individual gratings are projected, the subject detects them with a possibility of A and B respectively. According to probability summation when the two gratings are projected together (so there is a compound grating) the probability of seeing the compound grating is given be the formula

$$P_C = P_A + P_B(1 - P_A)$$

where the P_C is the probability of the compound grating to be visible, P_A is the probability of the A single grating and P_B the probability of the B individual grating. The possibility of seeing the compound gratings is always grater than the possibilities of the A and B gratings. If the two channels are

independent, it is found that the compound grating is slightly more visible by a factor of ~x1.2 (Stromeyer and Klein 1975; Watson and Nachmias 1980; Watson 1982).

1.3 Purpose of this study

The aim of this study is to evaluate spatial sensitivity using compound gratings projected at threshold and supra-threshold contrast. Using several combinations of spatial frequencies and several intervals of contrast between the two components, the contrast sensitivity will be measured. The results will allow us understand how the visual system responds at complex gratings. Neural channel interaction may be estimated according the results of this experiment and an index of this interaction will be calculated.

2.0 CHAPTER 2. METHODOLOGY

In the second chapter of this study the technical equipment used and the procedure of the experiments which figured for the purposes of this study will be described.

2.1 Technical equipment

The technical equipment used for the accomplishment of the experiments is consisted of a high resolution FD Trinitron ® SONY© GDM F520 CRT monitor, a high resolution VSG 2/5 (Cambridge Research Systems©) visual stimuli generator, a CB6 (Cambridge Research Systems©) infrared remote control and the NewRT (designed by Dr Neil R.A. Parry©) software. The monitor is a 21 inches high resolution screen at 864x602 pixels and the frequency rate is 120Hz. The graphic card is specially designed for vision experiments and its' output resolution is 15bit per any of the three colour channels (Red, Green, Blue). The remote control is designed for psychophysical experiments and the communication with the hosted PC is made via infrared radiation. The NewRT© software is developed to generate a wide range of stimuli for any kind of psychophysical experiments. It is possible to control any factor of the stimulus, from contrast and size to type, luminance standard deviation, spatial frequency etc.

The software is installed at a hosted PC (Windows© XPpro) and at the same computer the remote control is connected. The PC and the GDM F520 monitor are connected to the VSG graphic card. The parameters of the stimuli are specified to NewRT and via the graphic card are projected to the screen.

To be accurate the measurements the screen has been calibrated before the initiation of the experiments to be sure that prescribed contrast and luminance are the same as contrast and luminance of the visual stimulus.

For the calibration procedure a PR650 SpectraScan® Colorimeter (Photo Research Inc.), a ColourCal® Colorimeter (Cambridge Research Systems©) and the NewRT software were used. First, the gun voltages for the R, G and B colour channels were adjusted to 1 and a gamma by testing 128 voltages for each channel was obtained using the ColourCal®. The gamma represents a numerical parameter that describes the nonlinearity of intensity reproduction and this is due to the electron guns of a CRT display. x=0.31, y=0.316 and L=12.5cd/m^2 coordinates of the CIE system were settled to the software to be displayed at the monitor and the R, G and B values were noted. Then, the screen was measured with the PR650 and the x, y and L coordinates were adjusted until the SpectraScan® Colorimeter reads x=0.31, y=0.316 and L=12.5 and the new R, G and B values were recorded (see table 1).

The difference in the measured values from the adjusted, indicate that the R, G and B factors equal to 1 did not correspond the right factors. The ratios of the post over the pre adjustment values are the right scale factors and these were entered to the VSG software as the new R, G and B scale factors. With these new values a new gamma correction was obtained with ColourCal® and then the screen was measured to be sure that the PR650 reads the settled x, y and L coordinates to the software.

Figure 2.1 The technical equipment used for the experiments and the calibration of the monitor. PR650 (left), ColourCal (right) and the screen.

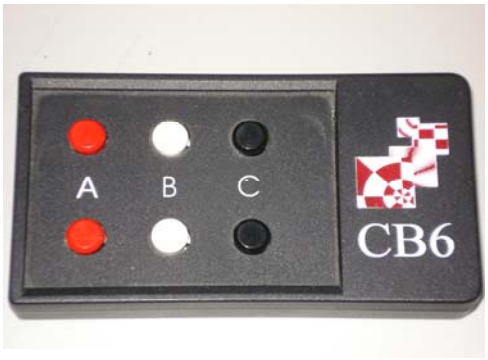

Figure 2.2 The CB6 remote control

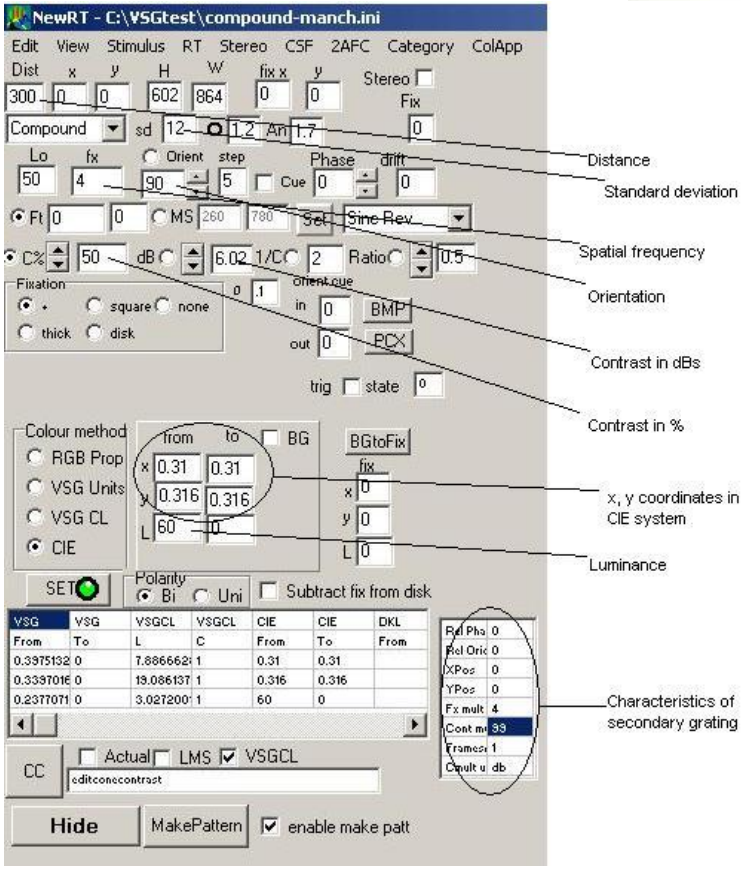

Figure 2.3 The NewRT software used for the generation of the stimuli. It is allowed to settle all the characteristics of the stimuli from the interface.

	x	y	L(cd/m^2)
Adjusted Values	0.311	0.323	12.8
Difference	+0.001	+0.07	+0.3
	R	G	B
Pre Adjustment	0.0762	0.0536	0.0487
Post Adjustment	0.0757	0.056	0.0474
Ratios (pre/post)	1.01	0.96	1.03

Table 2.1 The adjusted to NewRT x, y, L coordinates (upper table). The pre and post adjustment R, G, B values and the ratios values were used finally as the new R, G, B scale factors (lower table).

Screen luminance over time was measured to ensure that is constant during the experiments. In figure 2.4 the monitor luminance as a function of time is plotted and it can be seen that initially luminance is higher, decreasing over time until about the 70th minute, following an exponential decay. This points that the experiments need to initiate after this period to avoid any unwilling effect of luminance change (see figure 2.4). Screen luminance was also measured for a wide range of values. In figure 2.5 is the measured luminance as a function of the adjusted luminance at the software and in figure 2.6 the difference between the adjusted and the measured luminance (see figures 2.5, 2.6). It can be seen that the monitor luminance appears linear as a function of the adjusted luminance at the software. The percentage error for the luminance used to our experiments (60cd/m^2) is about 1.6%

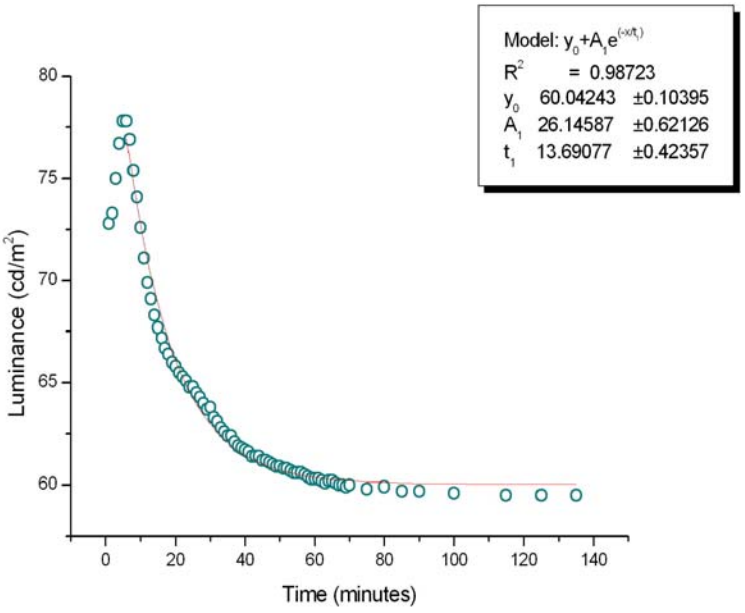

Figure 2.4 Measured luminance as a function of time after switching on the monitor

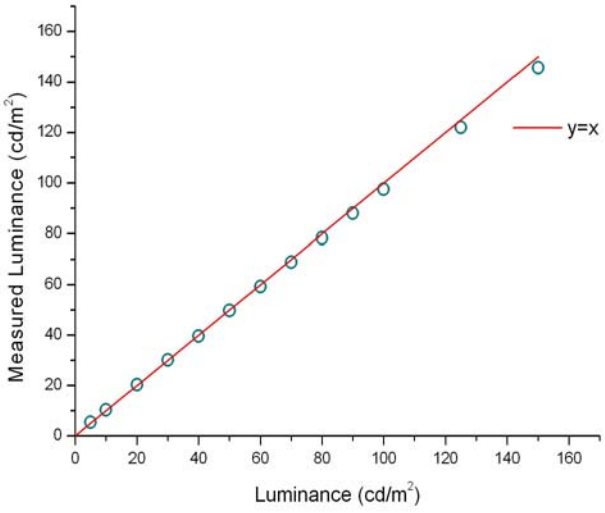

Figure 2.5 Measured luminance as a function of adjusted luminance.

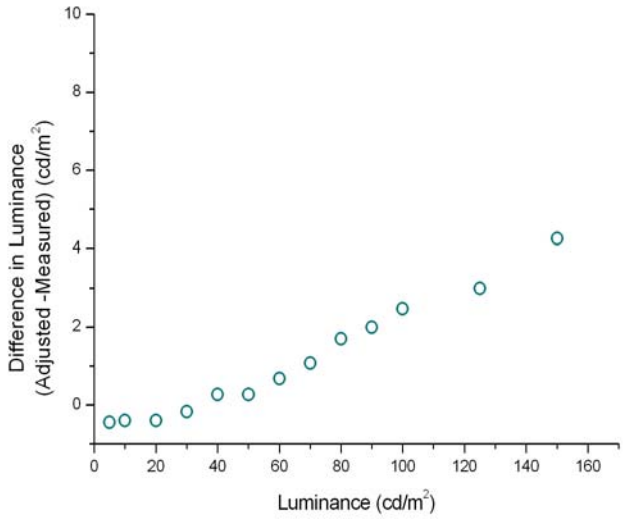

Figure 2.6 ΔL as a function of adjusted luminance

2.2 Stimuli

The stimuli were simple and compound gratings composed of one or two spatial frequencies respectively. For the compound gratings the main spatial frequency was always f=4c/deg and the secondary frequencies were 1.125f, 1.25f, 1.5f, 2f, 3f and 4f at viewing distance equal to 300cm. The simple gratings were at 4, 4.5, 5, 6, 8, 12, 16 c/deg. In the outer 5 degrees of the stimulus, a symmetrical cosine modulation of standard deviation equal to 12 was used to diminish edge effects.

As referred above, specially developed software was used to produce the stimuli. Many modern visual stimuli generators can produce such compound stimuli but usually introduce a reduction of the physical contrast of a x2 factor. With this specific software, the gratings are added pixel by pixel but then the individual contrast must be halved so that there will always be a x2 factor ratio between the contrast of the generated compound gratings and the contrast of the individual gratings. Figure 2.7 describes the technique used to generate compound gratings (see figure 2.7).

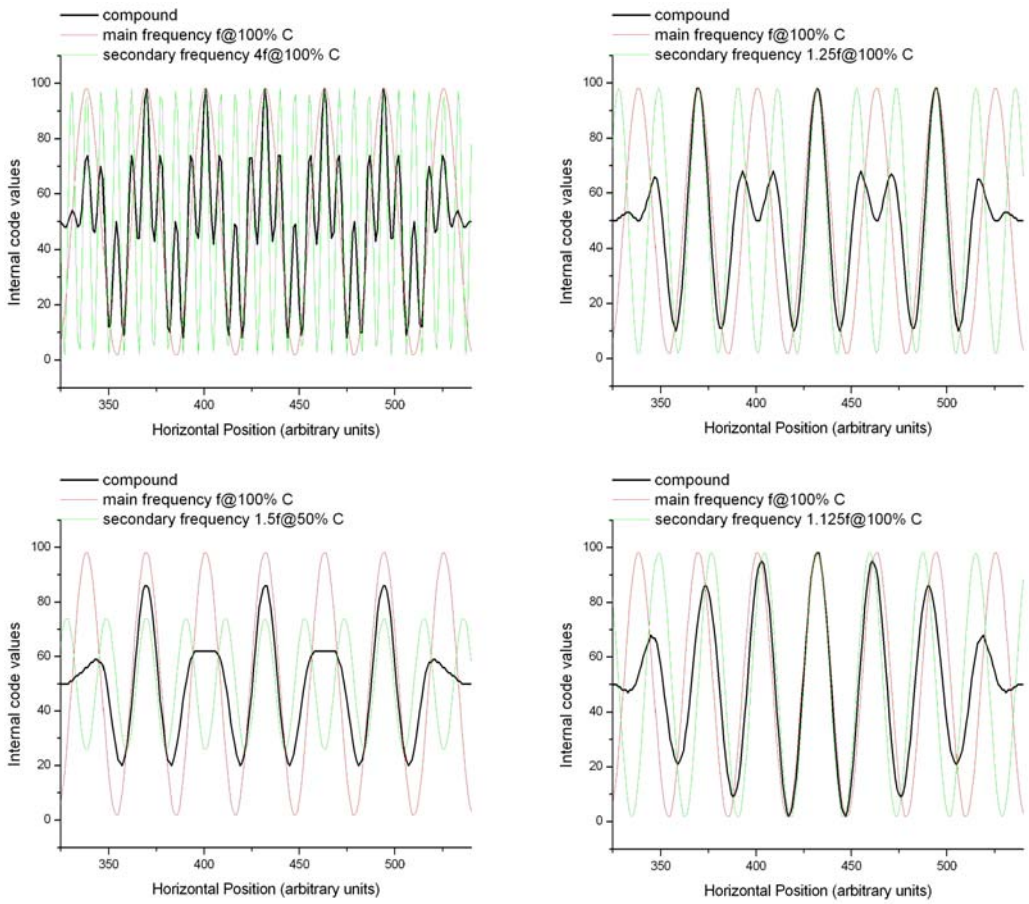

Figure 2.7 Example of frequency pairs added by the software. The value of y axis is at the internal values used by the program and does not correspond to luminance of the gratings. The physical contrast cannot be measured from these graphs, but the ratio of the component contrast can be calculated (i.e. at left bottom graph the peak-to-valley length of the secondary frequency is 50 internal values and the peak-to-valley length of the main frequency is 100 internal values. This corresponds at the contrast ratio of the 2 simple gratings which is 0.5)

2.3 Subjects

Five observers (NRAP, IJM, SP, TG and TP) where tested, all with prior experience in psychophysical experiments. NRAP, IJM, SP and TP are 47, 54, 37 and 27 years old men respectively, and TG is a 26 years old woman. All subjects were best corrected for the distance at which the experiments took place and with normal vision without any pathological disorders. The data collected from the dominant eye of each subject. The room was darkened and normal pupils were used. The mean screen luminance was 30cd/m^2 and the subjects were adapted for 5 to 10 minutes before the start of the experiments at that luminance.

2.4 Experiments

In this section the designed experiments for this work will be described. Two sets of experiments were conducted; both for evaluating threshold performance using compound gratings. A third experiment was figures to evaluate supra-threshold performance.

2.4.1 Control experiment

To confirm that the assumption of adding two gratings together results in a x2 reduction of the physical contrast was valid for our data, a pair of 4c/deg plus 4/deg gratings was tested and the threshold for the compound grating was determined. The orientation of both components was 90º.

2.4.2 Experiment 1. Threshold performance

The first experiment of this work was conducted to investigate the effect of adding two spatial frequency gratings in two different contrast conditions.

First of all, the spatial frequency of the main component was always 4c/deg and the spatial frequency ratios were 1.125, 1.25, 1.5, 2, 3, 4, 6 and in some cases 8. Both components had vertical orientation (90º). The subject had to set the threshold for four conditions for all of the spatial frequency pairs. The method used for determining the contrast threshold was the method of adjustment and the criterion for the threshold left free at the subject. Let C_1 and C_2 be the contrast of the primary and the secondary component respectively. The subject first was setting the threshold for the compound grating consisted of two components of 4c/deg. Secondary, a compound grating was projected with the main spatial frequency of one component at 0 contrast so that only the spatial frequency of the secondary component was visible and this is named C_2=1 condition. After, the C_1=C_2 condition was presented at the monitor where the primary and the secondary spatial frequency components were added at equal contrast. Finally, the two gratings were added with a difference in contrast. The difference in contrast was equal to the difference between the contrast thresholds of the individual gratings. So, the two gratings during this condition were supposed to be equal detectable since they were presented at their own individual threshold. This is the called C=θ condition where θ is the difference (in dB) in contrast. The subject was repeating the experiment four times for all the spatial frequency pairs and an average of three measurements was used (the first recording was always excluded). Prior and following the experiment the contrast thresholds of the individual gratings were assessed and at the begging of each pair the threshold for the compound grating consisted of two 4c/deg components was measured.

2.4.3 Experiment 2 – Threshold and sub-threshold performance

The second experiment of this study is at threshold performance and is designed to determine how the visual system is governed of spatial frequency channels. Many previous works compared pairs at each side of the peak of the contrast sensitivity function. In this work, only pairs from one side of the CSF (>4c/deg) were selected and this because it is known that different underlying mechanism govern at each side of the CSF. The spatial frequency of the two components of the compound gratings were the same as the previous experiment with the pairs in some cases ranging by two octaves. Compound gratings were generated by adding the component gratings in different contrast ratio to explore the relationship between the sensitivity to the compound grating and the physical contrast of the compound grating. While one component was at threshold the other one was sub-threshold and vice versa until projected at equal contrast. For example, lets consider a compound grating consisted of two components of 4c/deg and 6c/deg. The experiment was initiated with the determination of the threshold of the compound grating while the secondary component had an initial contrast difference of about 30dBs from the primary and so was invisible. This contrast difference was reduced with a step of 3dBs until the two components had a difference of 0dB and always the threshold of the primary component was determined. At the same session, the vice versa was occurred, which means that the threshold for the secondary component was adjusted while the primary one had a contrast difference from 30dBs to 0dBs. This procedure was repeated for each pair of spatial frequencies and in some cases, pairs of a ratio less than 1 were used for reasons that will be explained in following chapters. An average of three measurements was used.

Calculating the relative contrast of each grating, which is the threshold of the grating during the experiment over the contrast threshold of the individual spatial frequency grating summation contours were obtained.

2.4.4 Experiment 3. Supra-threshold performance

The third experiment of this study evaluated supra-threshold performance. In this experiment the discrimination of combined patterns was the object of research.

Compound gratings were projected while the contrast of the two components was laying out at a wide range. The two components were presented at a range of supra-threshold as well as sub-threshold contrasts. That means that while the one component of the compound grating was presented at sub-threshold contrast, the other component could be presented at supra-threshold or sub-threshold values and vice versa. The step was 2dB. So, the patterns projected were:

-The first individual component, while its contrast was supra-threshold and the contrast of the secondary component was sub-threshold,

-The second individual component, while its contrast was supra-threshold and the contrast of the primary component was sub-threshold,

-The compound grating consisted of the two components, while the contrast of the two components were supra-threshold, and

-Gratings, while the contrasts of the two components were sub-threshold.

The observer had not to adjust threshold but decide which pattern was presented at the screen. So, there were four options for the subject and in each of these options a different button was pressed:

1) Seeing the low spatial frequency component (primary), (press upper A button)

2) Seeing the high spatial frequency component (secondary), (press low A button)

3) Seeing both components, so the compound grating was present, (press upper C button)

4) Seeing nothing (press low C button).

The answers were given by the CB6 remote control and so a matrix with all the answers of the observer was obtained for a wide range of spatial frequencies. The spatial frequency of the primary component was always 4c/deg, as in previous experiments, while the spatial frequency of the secondary component was either at the side of the high spatial frequencies of the CSF or at the side of the low spatial frequencies.

3.0 CHAPTER 3. RESULTS

Three sets of experiments were conducted. First, results from the 'control' experiment are presented. Next, the results of the Experiment 1 described at the previous chapter and the results of the second experiment are referred. Finally, some graphs derived from the third experiment are presented.

3.1 Control experiment

Subjects IJM and TP participated in a control experiment while a compound grating of 4c/deg plus 4c/deg was projected in two contrast conditions. The first one with 0dB contrast difference, which mean that the two components were at equal contrast. In the second experiment there was 99dB contrast difference between the two components, which mean that one component was invisible. In table 3.1 there are the results for the two subjects.

IJM					TP				
#	Int (dB)	Main	Fx mult	dB	#	Int	Main	Fx mult	dB
1	99	4	1	40	1	0	4	1	47
2	0	4	1	46	2	99	4	1	41
3	0	4	1	47	3	0	4	1	46
4	0	4	1	49	4	0	4	1	47
5	0	4	1	46	5	99	4	1	41
6	99	4	1	41	6	0	4	1	47
7	0	4	1	46	7	0	4	1	45
8	99	4	1	39	8	0	4	1	46
9	0	4	1	45	9	99	4	1	41
10	99	4	1	39	10	99	4	1	41
11	99	4	1	38	11	0	4	1	46
12	99	4	1	38	12	99	4	1	41
13	99	4	1	38	13	99	4	1	41
14	99	4	1	40	14	0	4	1	46
15	99	4	1	38	15	0	4	1	46
16	99	4	1	38	16	99	4	1	40
17	0	4	1	44	17	99	4	1	41
18	0	4	1	43	18	0	4	1	46
19	0	4	1	44	19	99	4	1	41
20	0	4	1	45	20	99	4	1	42

Table 3.1 Results of the Control Experiment

The average contrast threshold for each condition is shown in table 3.2:

	99dB	0dB	Difference
IJM	38.9	45.5	6.6
TP	41	46.2	5.2

Table 3.2

The difference between the two contrast conditions is 6.6dB and 5.2dB for subjects IJM and TP, respectively. We have to remind that theoretically a 6dB difference corresponds to a ratio of 2. To be sure that the difference between the two conditions does not differs from the theoretical value of 6dB, a t-test was performed and found that $p>0.05$ ($a=0.05$).

3.2 Experiment 1. Threshold performance

The results of the first experimental procedure are shown graphically below (see figure 3.1-3.5). At the lower x axis the spatial frequency ratio and at the upper x axis the corresponded spatial frequency in c/deg are drawn. The multiplier factor is 4 as the 4c/deg spatial frequency is the main frequency used in our experiments. Y axis plots the contrast sensitivity (in dB). At the lower graph the difference in contrast sensitivity is depicted. C_1 and C_2 are the contrast of the first and the second component of the compound gratings, respectively. The open green triangles correspond to the data of a compound consisted of always two single 4c/deg and 4c/deg gratings was presented at the screen. The secondary component was at 99dB contrast difference from the primary grating and so only the primary 4c/deg component was visible. This is the condition where $C_1=1$ and $C_2=0$ were used in order to examine the sensitivity for the first component. The $C_1=0$ and $C_2=1$ (filled squares with the straight line) is the condition in which the secondary component of the compound grating was 1.125f, 1.25f, 1.5f, 2f, 3f, 4f and 6f where f is the 4c/deg spatial frequency of the primary

component. So, at this condition the components of i.e. 4.5c/deg, 5c/deg, 6c/deg, 8c/deg, 12c/deg, 16c/deg and 24c/deg were added with the primary being at 99dB contrast difference from the secondary. This condition was tested in order to examine the sensitivity for the second component, as the first was well sub-threshold. The filled dark cyan circles with the straight line is the C_1=C_2 contrast condition where the primary 4c/deg component and the secondary 1.125f, 1.25f etc component were presented at equal contrast. The last condition is the C_2=θ where the physical contrast of the secondary component was adjusted accordingly so that both components where equally visible according to their respective thresholds. For example, if the main spatial frequency grating had a contrast threshold at 50dB and the secondary grating at 40dB, θ equals 10dB and so the secondary component had to be added to the primary with a contrast difference equal θ in order both components being equally visible at threshold. The θ and equal elevation is the C_2=θ minus the C_2=1 condition and the C_1=C_2 minus the C_1=1 condition, respectively. For all subjects, in the C=θ condition less contrast is needed to be detected from the C=0 condition and the C=1 and 4c/deg conditions show the same sensitivity.

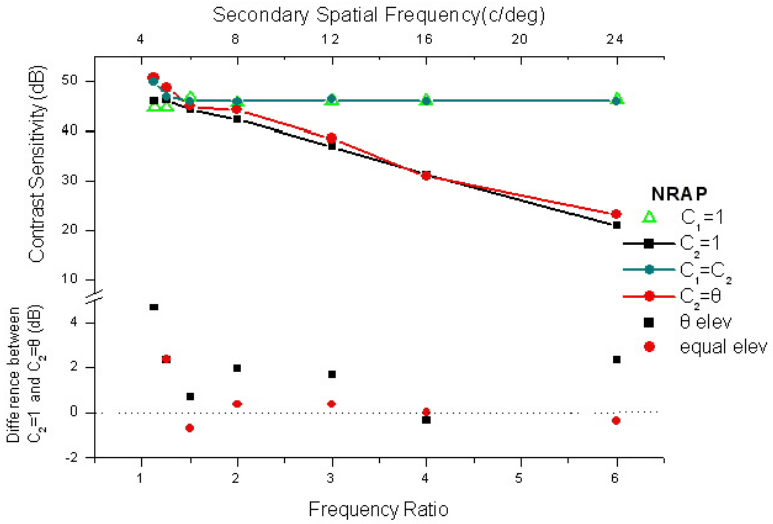

Figure 3.1 Subject NRAP. Lower x axis plots the frequency ratio (secF_x/primF_x=ratio), upper x the spatial frequency in c/deg for the secondary component and the y axis plots the contrast sensitivity (in dB). The lower graph is the difference between the C=θ and C=0 condition.

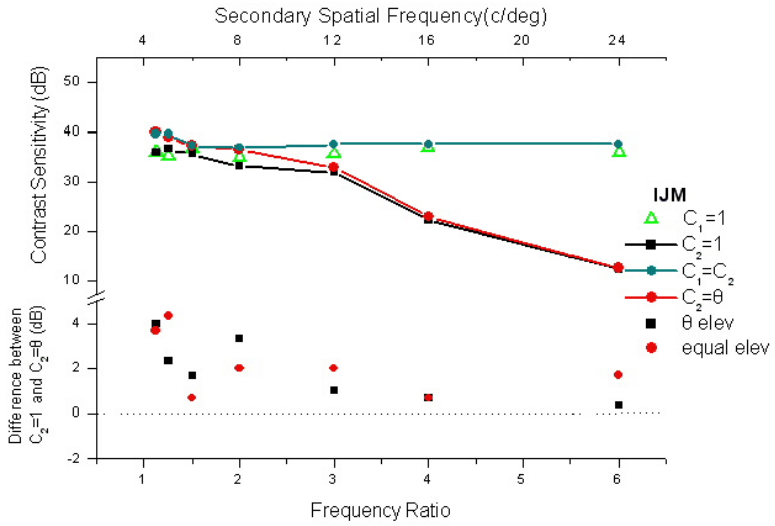

Figure 3.2 Subject IJM. Same as in figure 3.1

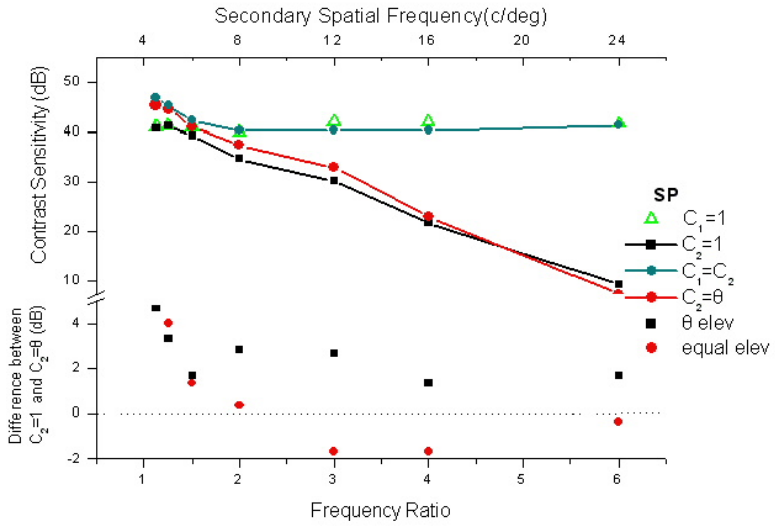

Figure 3.3 Subject SP. Same as in figure 3.1

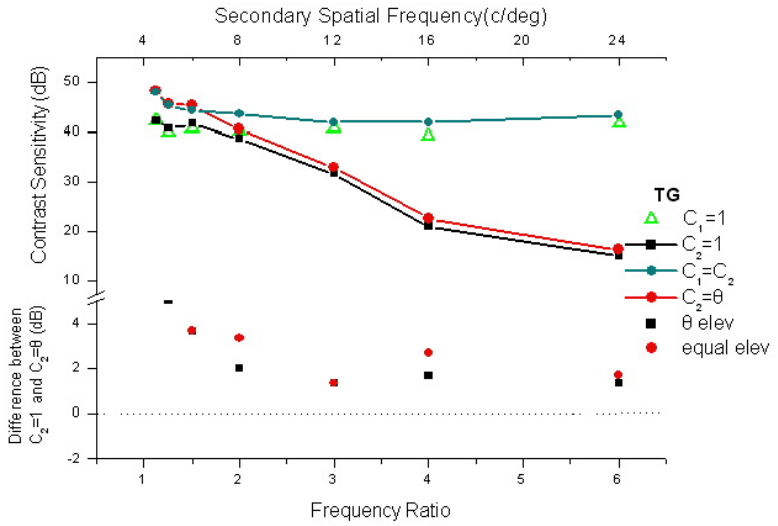

Figure 3.4 Subject TG. Same as in figure 3.1

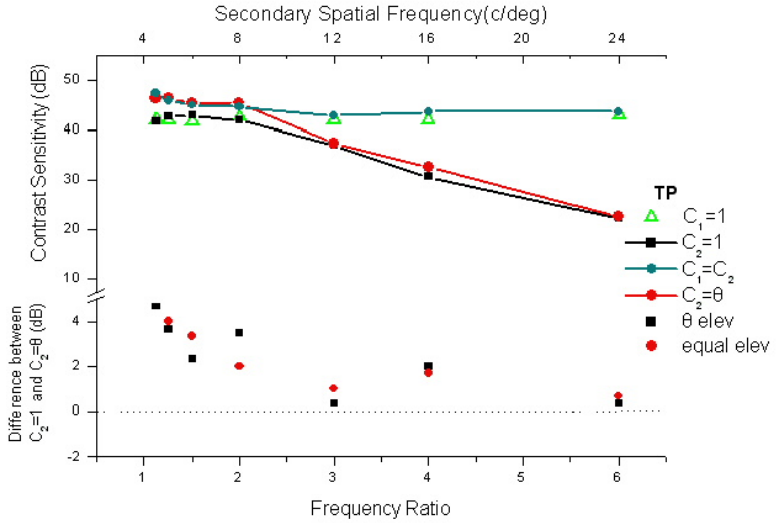

Figure 3.5 Subject TP. Same as in figure 3.1

The difference between the C_2=θ minus the C_2=1 condition is shown graphically in figure 3.6 for all observers. Also, the average theta elevation derived from all subjects is plotted (see figure 3.6). For ratios lower than 2 the sensitivity is increased and finally falls for ratios greater than 2, reaching a plateau of 1.2dB.

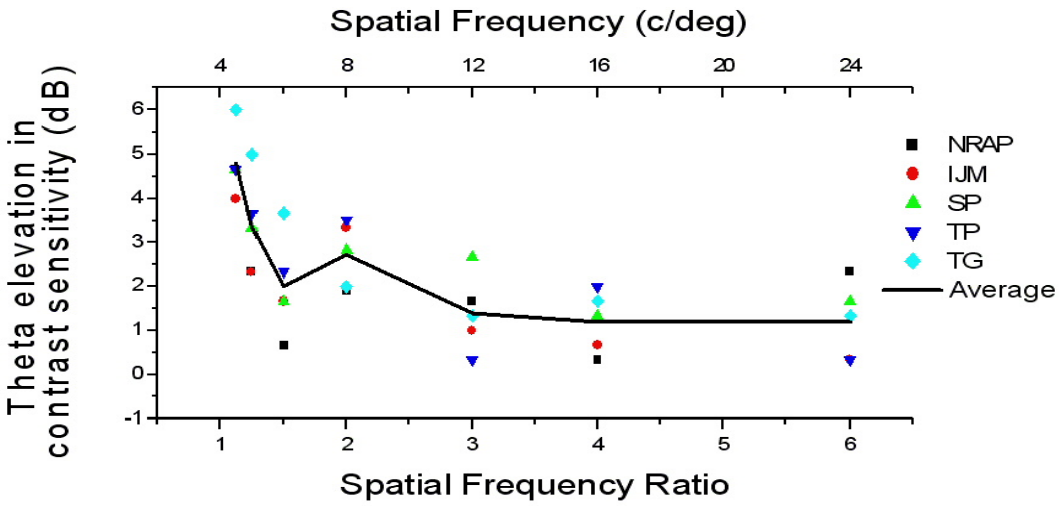

Figure 3.6. Theta elevations for all subjects. Lower x axis corresponds at spatial frequency ratio, upper x axis at spatial frequency in c/deg and y axis plots the difference in dB between the C_2=0 minus the C_2=1 condition.

3.3.1 Experiment 2. Threshold and sub-threshold performance

Contrast sensitivity was measured for compound gratings consisting of two single components, each of them in different relative contrasts. The relative contrast threshold was calculated by the contrast threshold of the compound over the contrast threshold of the individual component. The relative contrast threshold of the high spatial frequency component plotted as a function of the relative contrast threshold of the low spatial frequency component.. These graphs can provide an index of channel summation at various contrast levels (see figures 3.7-3.15 and discussion).

At the following graphs (see fufures 3.7-3.15) the summation curves are plotted for six different pairs of spatial frequencies for two subjects, TP (2 runs) and SP. The main component has a spatial frequency of 4c/deg while the spatial frequency of the other component varies from 4.5 to 16c/deg (i.e. the range of the spatial frequencies in octaves start from 2.17octaves and ends at 4 octaves). At x axis there is the relative contrast of the low spatial frequency which is always 4c/deg. At y axis there is the relative contrast of

the high spatial frequency component. Theoretically, a compound grating of two components would result to two (separate or not) spatial frequency tuned channels. If these channels where completely independent, the relative contrast for the low and the high spatial frequency would lie across the x=1 and y=1 lines respectively, and this because the two components would be detected independently. So the measured contrast threshold (C_m) would be equal to the contrast threshold of the individual grating (C_m^*) which would result to a ratio would be equal to 1 ($C_m/C_m^*=1$). If the two components are detected by a single spatial tuned channel (this happens only when the two components of a compound grating are identical), the sum of the relative contrast should be equal to 1, because only one value of contrast threshold can be detected by a single channel which mean that the sum of the relative contrasts should be equal to 1 ($\frac{C_{m1}}{C_{m1}^*}+\frac{C_{m2}}{C_{m2}^*}=1$). This means that the data points of this case should lie along a line described as x+y=1. Consequently, the data points of this experiment should lie somewhere along the x+y=1 line and x=1 and y=1 lines. A model which describe best these cases is the $\left(\frac{C_{m1}}{C_{m1}^*}\right)^a+\left(\frac{C_{m2}}{C_{m2}^*}\right)^a=1$ (equation 1), with the exponent a between 1 for complete summation and infinity for complete absence of summation (completely independent channels). A best fit procedure, according the above equation, done for all the frequency pairs and for both subjects. The curve fitting performed with MATLAB® using least squares for non linear curves method. The results are shown in graphs 3.7 to 3.15 where the value of a is depicted at the top of each graph. As discussed, there are two runs for each spatial frequency pair for subject TP (graphs 3.7-3.12) so the value of a is derived also using all data points (graphs 3.13 - 3.15). The minimum value of a calculated in this experiment is 1.06 and as expected was found for the compound grating consisted of

4c/deg and 4.5c/deg components. The maximum value equals to 3.47 and derived from the compound grating of 4c/deg and 16c/deg.components

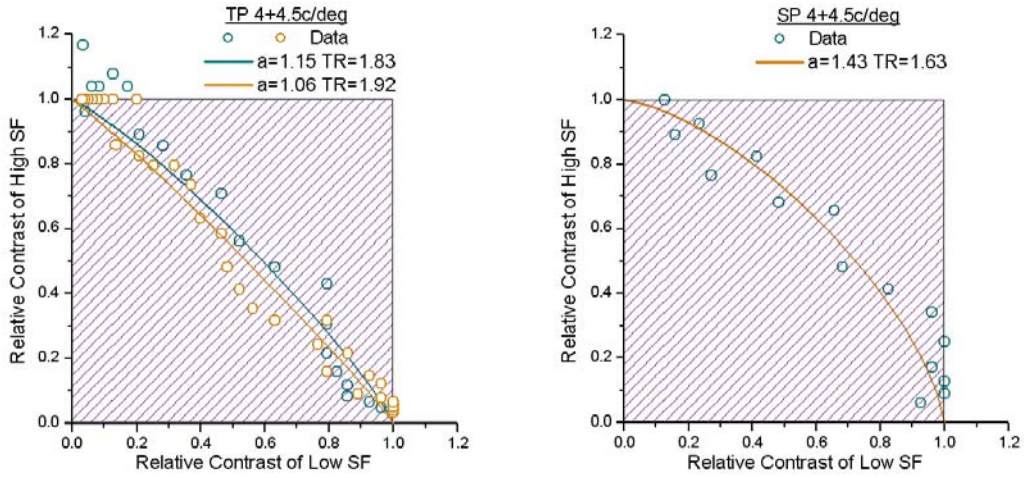

Figure 3.7 Frequency pair of 4&4.5c/deg. The x axis corresponds at the relative contrast threshold for the low spatial frequency component while the y axis at the higher spatial frequency component. Data from TP (left) and SP (right). See text for discussion on a and TR values

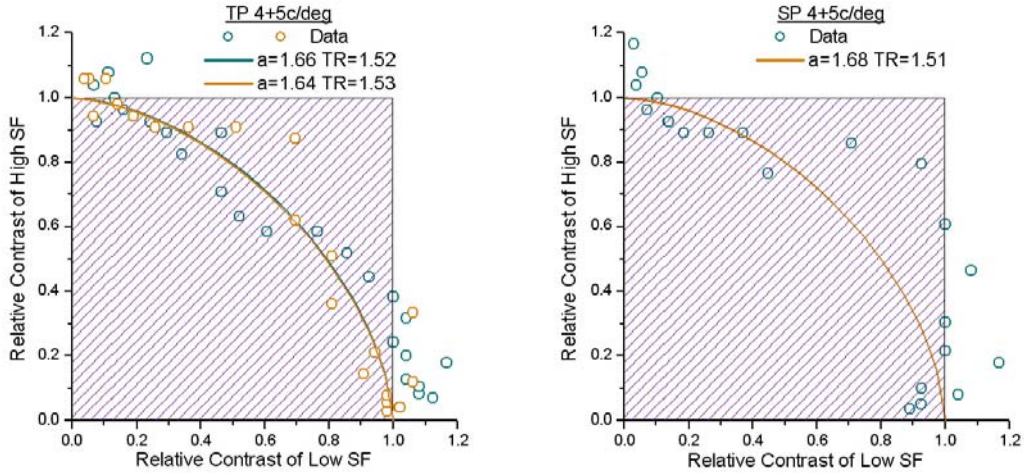

Figure 3.8 Frequency pair of 4&5c/deg. Same as in figure 3.7

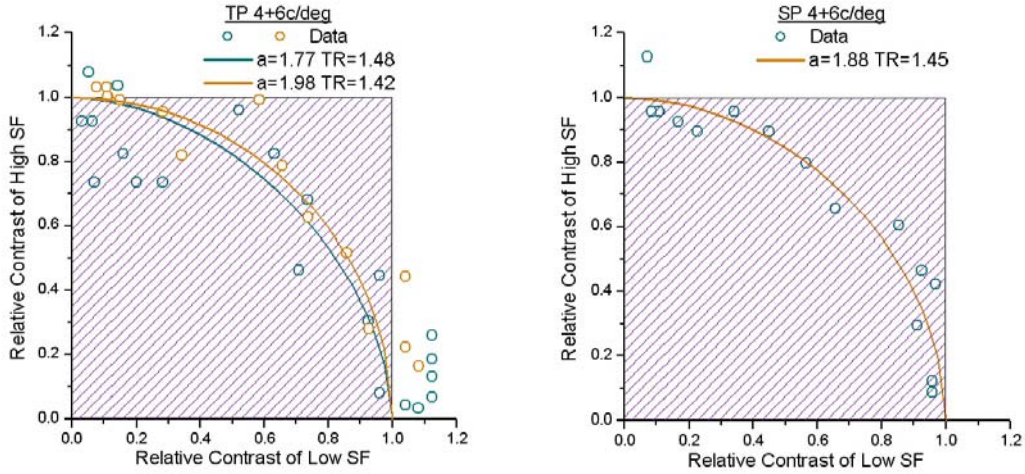

Figure 3.9 Frequency pair of 4&6c/deg. Same as in figure 3.7

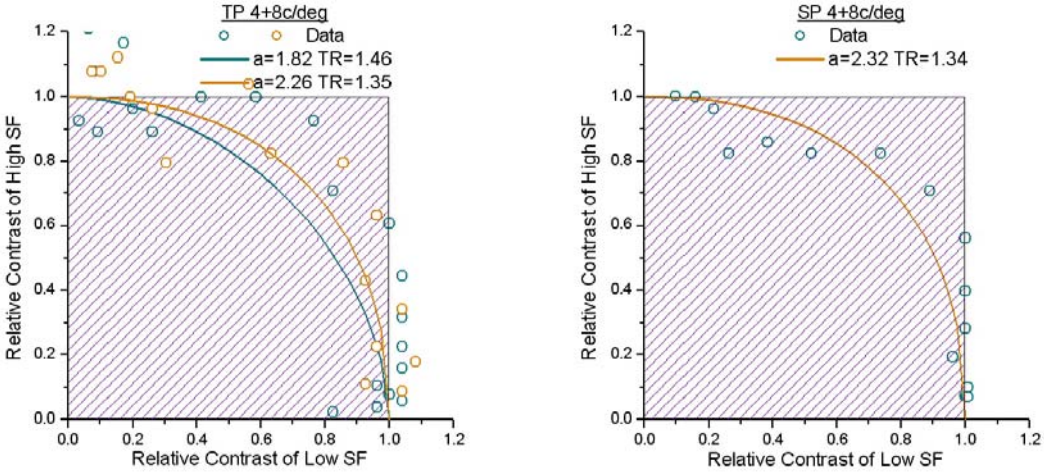

Figure 3.10 Frequency pair of 4&8c/deg. Same as in figure 3.7

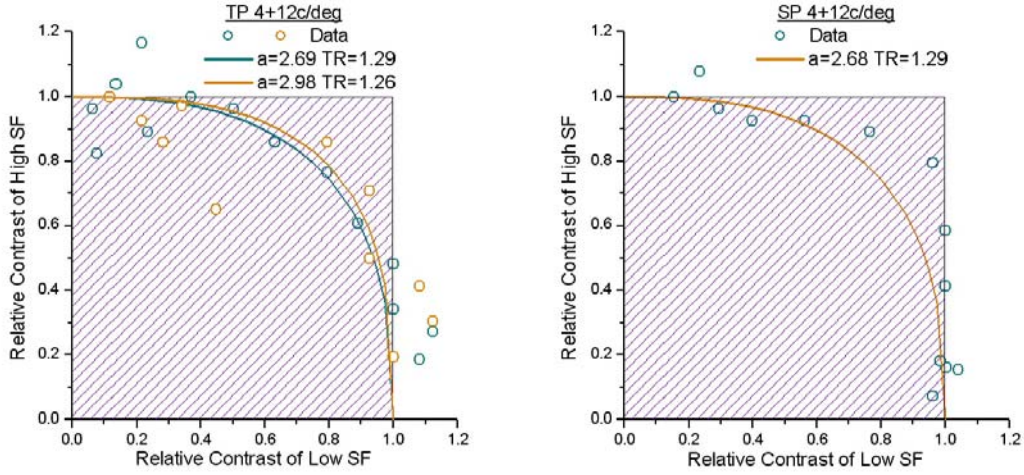

Figure 3.11 Frequency pair of 4&12c/deg. Same as in figure 3.7

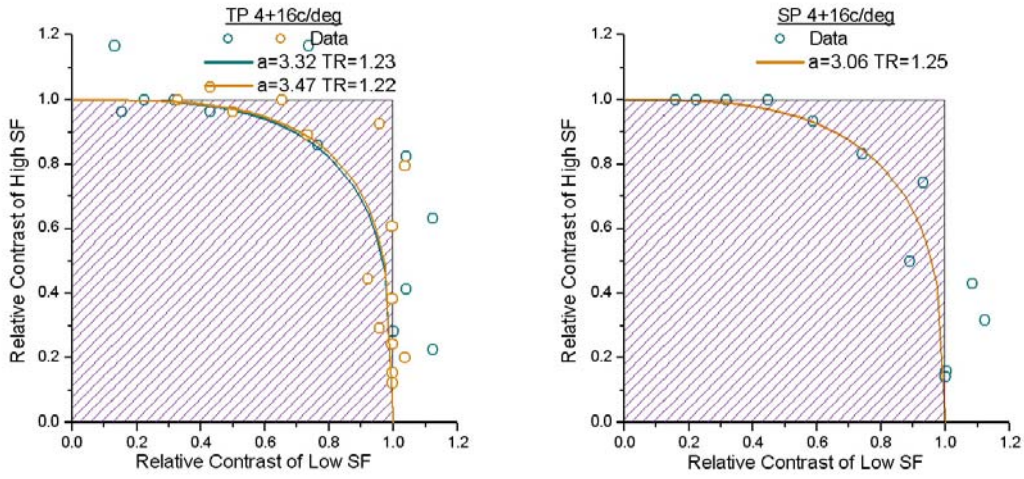

Figure 3.12 Frequency pair of 4&16c/deg. Same as in figure 3.7

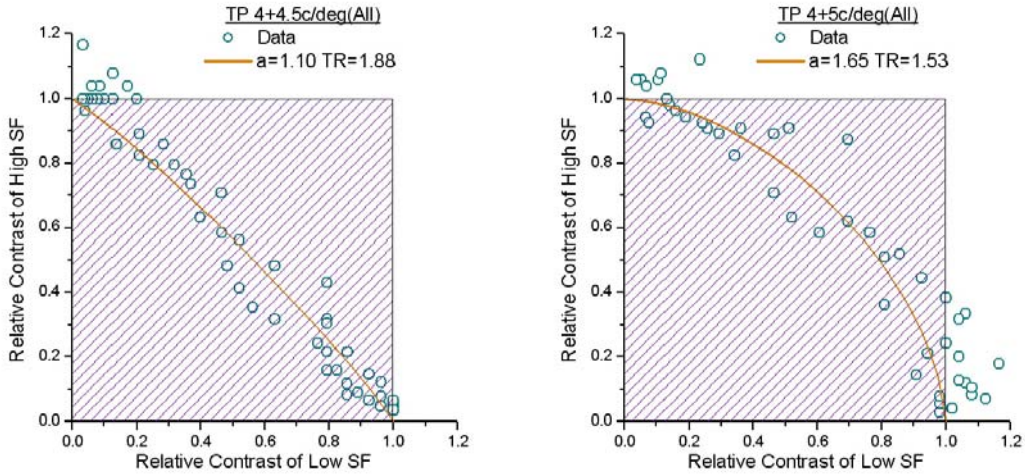

Figure 3.13 Frequency pair 4&4.5c/deg and 4&5c/deg. Data from two runs of TP, fitted together.

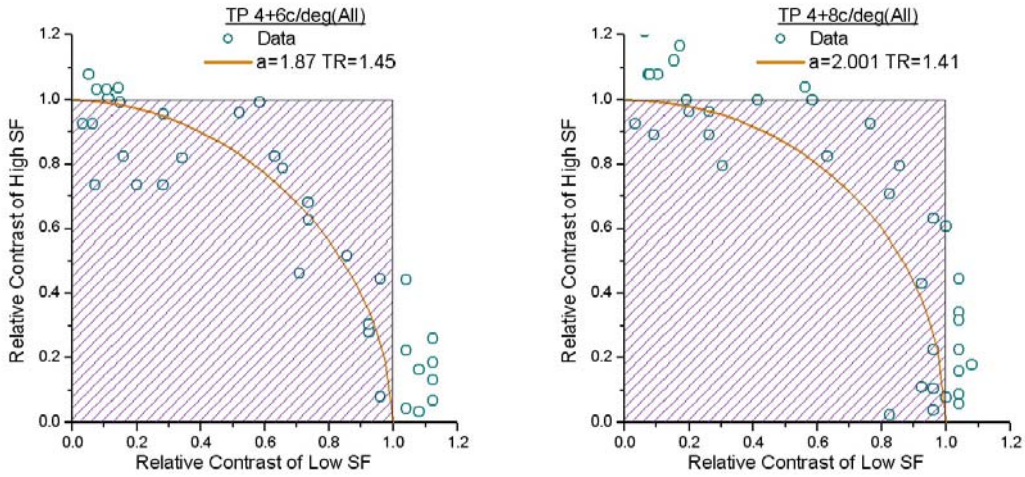

Figure 3.14 Frequency pair 4&6c/deg and 4&8c/deg. Same as in figure 3.13

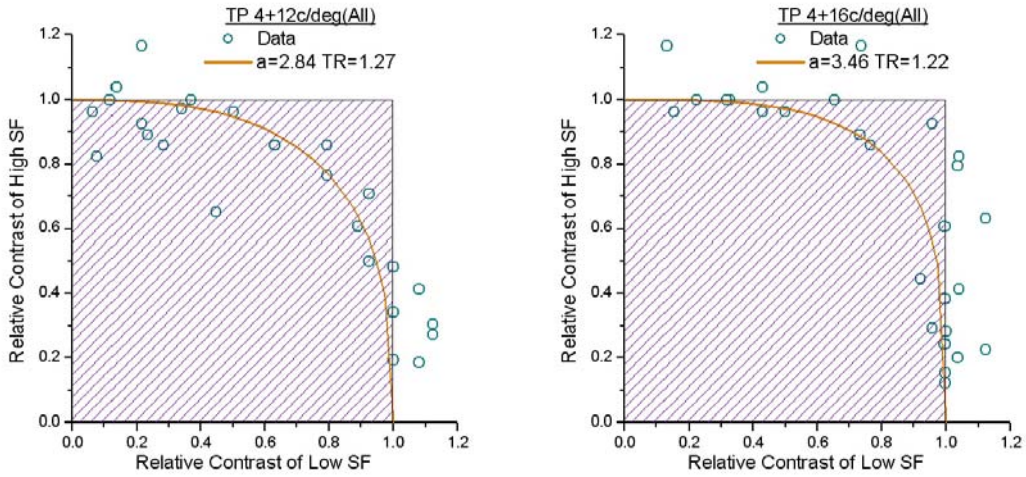

Figure 3.15 Frequency pair of 4&12c/deg and 4&16c/deg. Same as in figure 3.13

Another point of view of these data is of interest. Lets consider the y=x line which intersects at one point all the fitted curves. If there is complete neural summation the y=x line intersects the y+x=1 line (which describes complete summation) at x=y=0.5 (in units of relative contrast). The reciprocal of this value is 1/0.5=2. If there is complete absence of neural summation then the curves which describe this condition are the x=1 and y=1 and the x=y line intersects these curves at point x=y=1. the reciprocal of this value is also 1. A formula that fits these two data points is the $2^{1/a}$ where a is the exponent of equation 1. Indeed, if a is equal to 1 so that there is complete summation then $2^{1/1}=2$ which is the value calculated in previous lines for this condition. If a is equal to infinity, so that there is complete absence of summation then $2^{1/\infty}=1$ which is also the previous value calculated for this extreme condition. Let the $2^{1/a}$ called threshold ratio which is in fact the reciprocal of relative contrast at the point where the x=y intersects the curves. The threshold ratio is calculated for every pair of spatial frequency for both subjects. The value of the threshold ratio (TR) is shown in the graphs 3.7-3.15 at the upper right corner. In the graphs 3.16 and 3.17 the threshold ratio is plotted as a function of the secondary spatial frequency in octaves (see figures 3.16, 3.17).

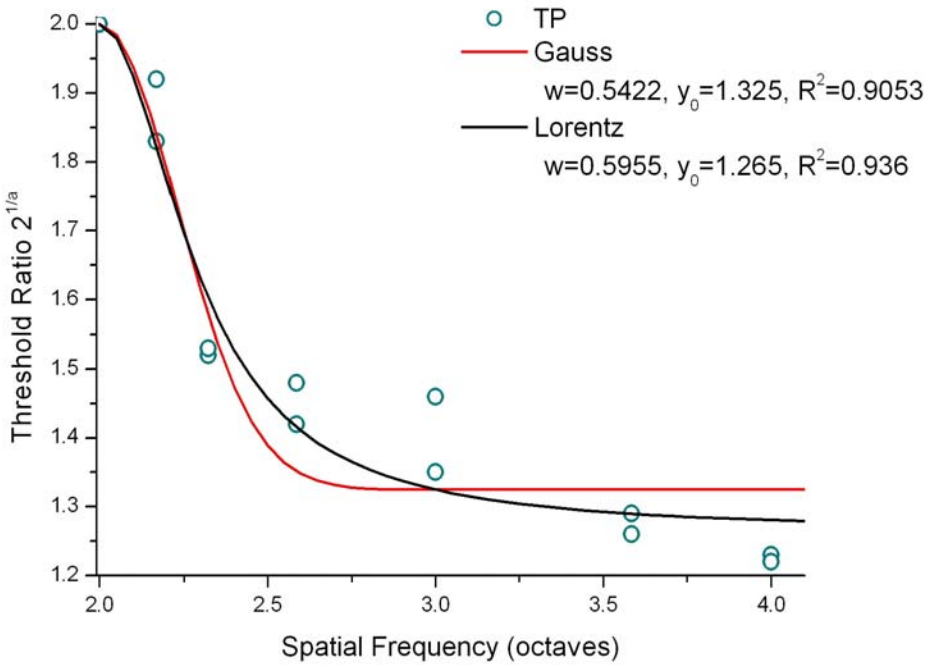

Figure 3.16 The threshold ratio as a function of the spatial frequency for data derived from TP. At x axis is plotted the spatial frequency in octaves and at y axis the threshold ratio $2^{1/a}$. The fitting done according two equations.

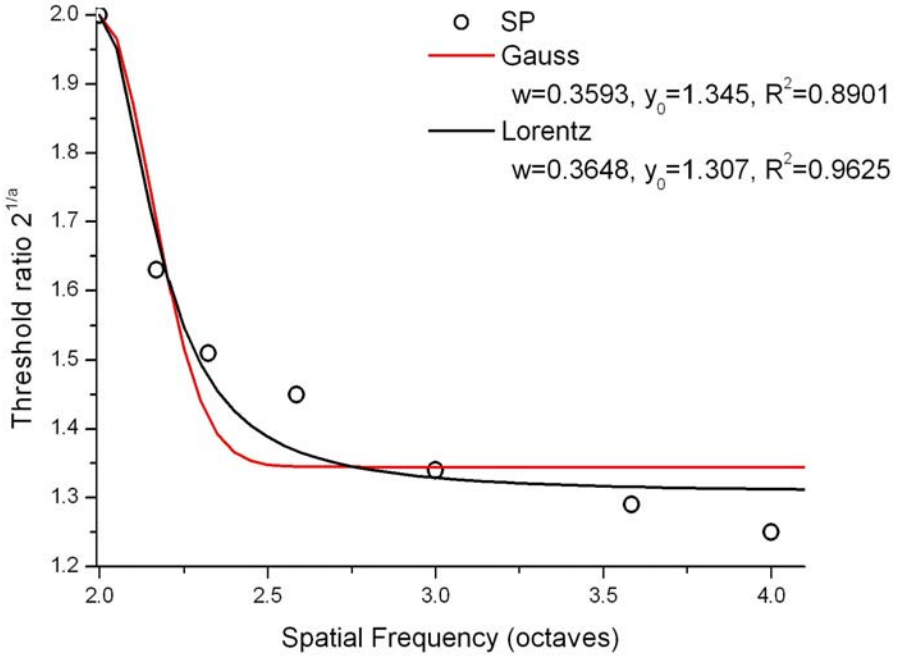

Figure 3.17 Same as in figure 3.16. Subject SP.

The above graphs (3.16, 3.17) may provide some information about the bandwidth of the 4c/deg channel. Under the assumption that the channel is symmetrical, curves fitted using non linear least square method in MATLAB®. The equations used are a Gauss and a Lorentz equation which are used for symmetrical data and also because the data show a peak.

$$y = y_0 + (y_c - y_0)e^{-\frac{2(x-x_c)^2 \ln 4}{w_1^2}} \quad \text{Gauss}$$

$$y = y_0 + (y_c - y_0)\frac{w^2}{4(x-x_c)^2 + w^2} \quad \text{Lorentz}$$

Under the assumption of symmetry, the Full Width at Half Maximum of these curves is the bandwidth of the entire channel. This value is calculated for the two above graphs and the results are shown in table 3.3.

	Bandwidth (Octaves)	Min SF (Octaves)	Max SF (Octaves)
TP	0.5955	1.70	2.30
SP	0.3648	1.81	2.18

Table 3.3 Channel Bandwidth in Octaves for both subjects

Previous results are shown graphically at next graphs (see figures 3.18, 3.19)

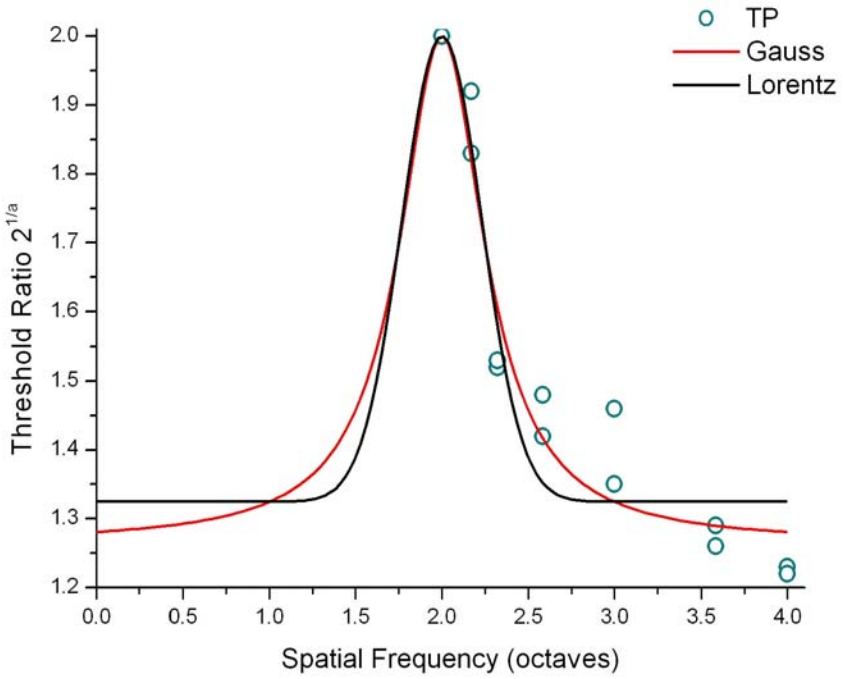

Figure 3.18 The 4c/deg spatial frequency channels for subject TP, under the assumption that the channel is symmetrical at both sides of the 4c/deg.

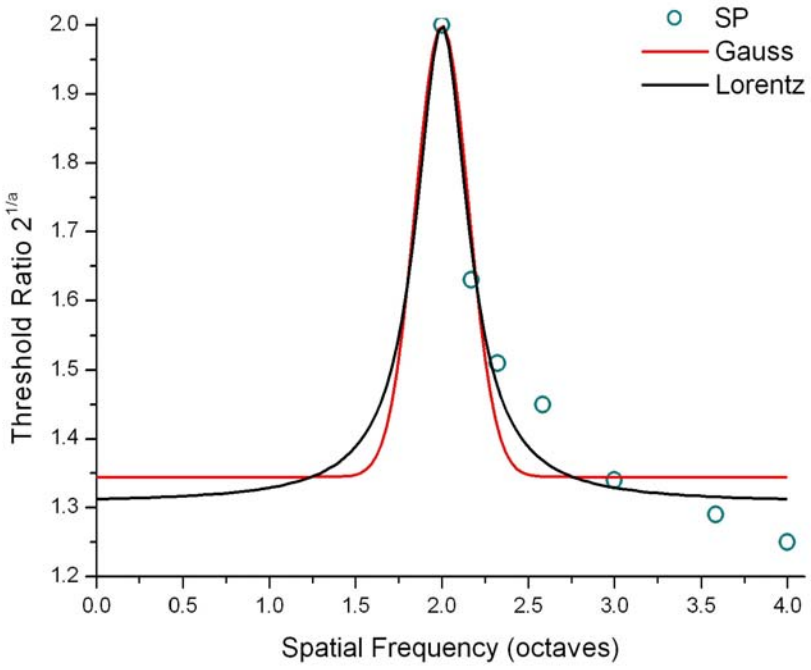

Figure 3.19 The 4c/deg spatial frequency channels for subject SP, under the assumption that the channel is symmetrical at both sides of the 4c/deg.

3.3.2 Experiment 2. Spatial frequencies lower than 4c/deg

The bandwidth of the channel centred at 4c/deg, calculated under the assumption that this neural channel is symmetrical at both sides of the central spatial frequency. The 4c/deg spatial frequency appears at the maximum of the CSF of the whole visual system and at one side, to higher spatial frequencies, the CSF falls almost linear but at the other lower side the CSF falls in a different mode and seems not to appear linearity. This appearance may be evidence that the visual system is mediated by different underlying mechanisms at the two sides of the CSF and this hypothesis propelled us to see what is happening if the secondary spatial frequency is lower than 4c/deg. Both subjects participated in a single session of the experiment using compound gratings with the spatial frequency of the secondary grating being 1c/deg (TP and SP) and 2c/deg (TP). The same procedure as in main experiment was followed and the results are shown in the graph below (see figure 3.20, 3.21).

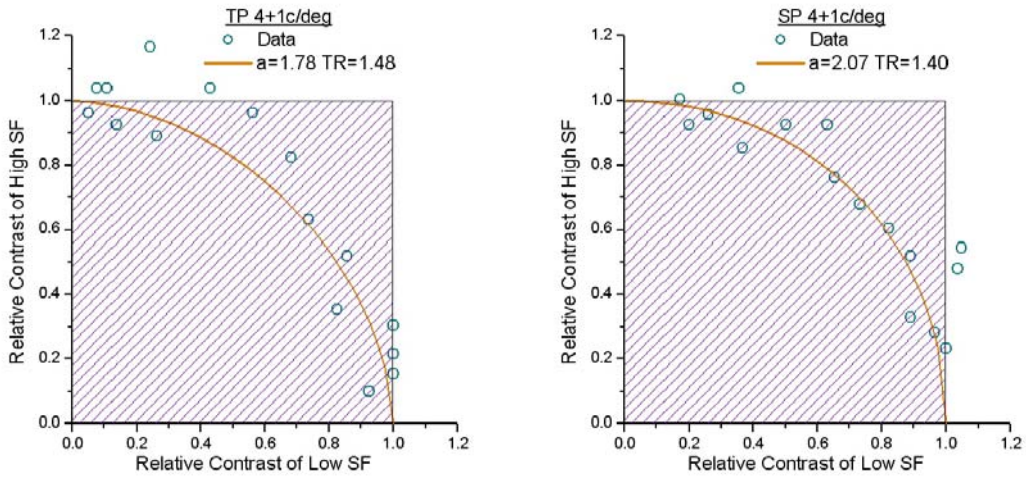

Figure 3.20 Frequency pair of 4&1c/deg (TP and SP)

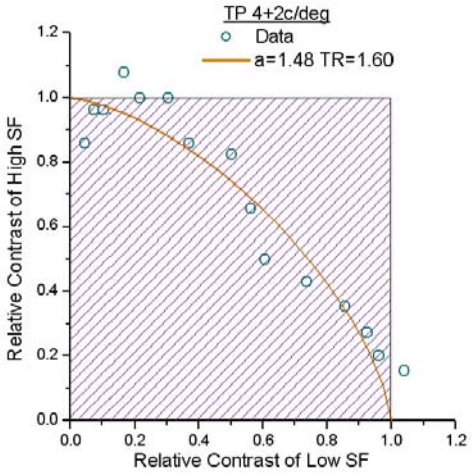

Figure 3.21
Frequency pair of 4&2c/deg (TP)

If we include the data points from the previous graphs in figures 3.16 and 3.17 the updated graphs are obtained (see figures 3.22, 3.23).

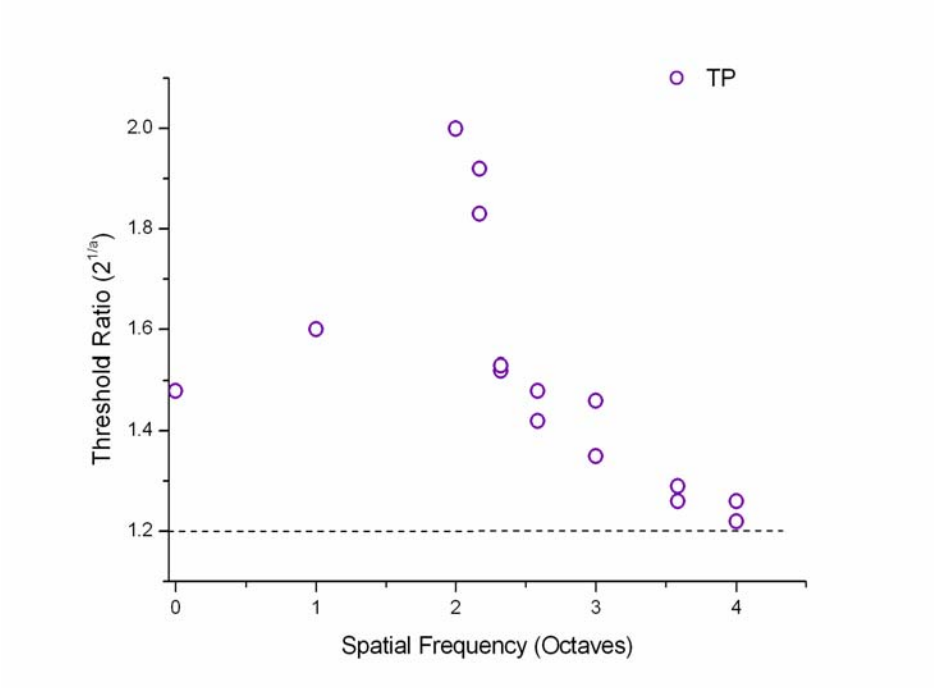

Figure 3.22 Threshold ratio as a function of secondary spatial frequency (TP 1c/deg and 2c/deg results added).

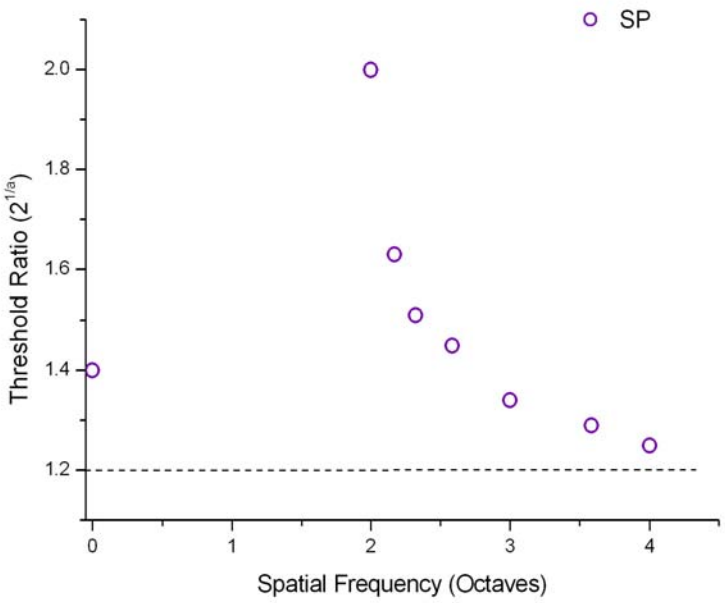

Figure 3.23 Threshold ratio as a function of secondary spatial frequency (SP 1c/deg results added).

The data at the side of the lower spatial frequencies are not enough to do a satisfactory curve fitting at the above graphs. But, a gross fitting with just two points from the side of lower spatial frequencies indicates an asymmetric fitting.

3.4 Experiment 3. Supra-threshold performance

Pattern discrimination was the object of the third experiment at a wide range of contrast values for both components of a compound grating. The results for observers TP and SP for some pairs of spatial frequencies are shown at the following 'matrices' (see figure 3.24-3.27). Any cell of the matrix has in fact two coordinates, x and y. The abscissa indicates the contrast of the high spatial frequency component and the ordinate corresponds at the contrast of the low spatial frequency component. For example a cell may has coordinates (35, 28) which means that when the experiment run this cell, the high spatial frequency component was at 35dB

contrast while the low spatial frequency component was at 28dB contrast. Any cell is filled with X, Y, B or 0. X letter indicates that the observer decided that detected the high spatial frequency component, while the experimental procedure was at the certain cell. Y letter indicates that the observer saw only the low spatial frequency component, B that saw both components which means that a compound grating was projected and 0 that he did not see anything.

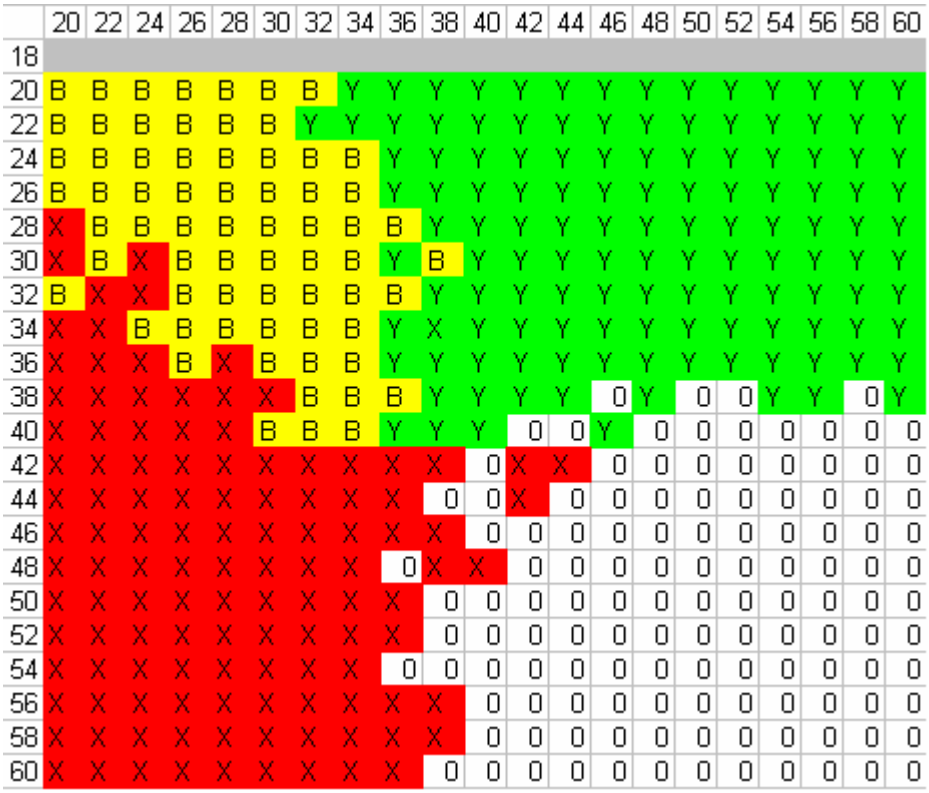

	20	22	24	26	28	30	32	34	36	38	40	42	44	46	48	50	52	54	56	58	60
18																					
20	B	B	B	B	B	B	B	Y	Y	Y	Y	Y	Y	Y	Y	Y	Y	Y	Y	Y	Y
22	B	B	B	B	B	B	Y	Y	Y	Y	Y	Y	Y	Y	Y	Y	Y	Y	Y	Y	Y
24	B	B	B	B	B	B	B	B	Y	Y	Y	Y	Y	Y	Y	Y	Y	Y	Y	Y	Y
26	B	B	B	B	B	B	B	B	Y	Y	Y	Y	Y	Y	Y	Y	Y	Y	Y	Y	Y
28	X	B	B	B	B	B	B	B	B	Y	Y	Y	Y	Y	Y	Y	Y	Y	Y	Y	Y
30	X	B	X	B	B	B	B	B	Y	B	Y	Y	Y	Y	Y	Y	Y	Y	Y	Y	Y
32	B	X	X	B	B	B	B	B	B	Y	Y	Y	Y	Y	Y	Y	Y	Y	Y	Y	Y
34	X	X	B	B	B	B	B	B	Y	X	Y	Y	Y	Y	Y	Y	Y	Y	Y	Y	Y
36	X	X	X	B	X	B	B	B	Y	Y	Y	Y	Y	Y	Y	Y	Y	Y	Y	Y	Y
38	X	X	X	X	X	X	B	B	B	Y	Y	Y	Y	0	Y	0	0	Y	Y	0	Y
40	X	X	X	X	X	B	B	B	Y	Y	Y	0	0	Y	0	0	0	0	0	0	0
42	X	X	X	X	X	X	X	X	X	X	0	X	X	0	0	0	0	0	0	0	0
44	X	X	X	X	X	X	X	X	X	0	0	X	0	0	0	0	0	0	0	0	0
46	X	X	X	X	X	X	X	X	X	X	0	0	0	0	0	0	0	0	0	0	0
48	X	X	X	X	X	X	X	X	0	X	X	0	0	0	0	0	0	0	0	0	0
50	X	X	X	X	X	X	X	X	X	0	0	0	0	0	0	0	0	0	0	0	0
52	X	X	X	X	X	X	X	X	X	0	0	0	0	0	0	0	0	0	0	0	0
54	X	X	X	X	X	X	X	X	0	0	0	0	0	0	0	0	0	0	0	0	0
56	X	X	X	X	X	X	X	X	X	X	0	0	0	0	0	0	0	0	0	0	0
58	X	X	X	X	X	X	X	X	X	X	0	0	0	0	0	0	0	0	0	0	0
60	X	X	X	X	X	X	X	X	X	0	0	0	0	0	0	0	0	0	0	0	0

Figure 3.24 A matrix derived from the supra-threshold experiment (TP). At x axis is the contrast of a 6c/deg component, y axis is the contrast of the 4c/deg spatial frequency component. X indicates that the observer sees the high spatial frequency, Y that sees the low spatial frequency, B that sees both components and 0 that he does not see anything.

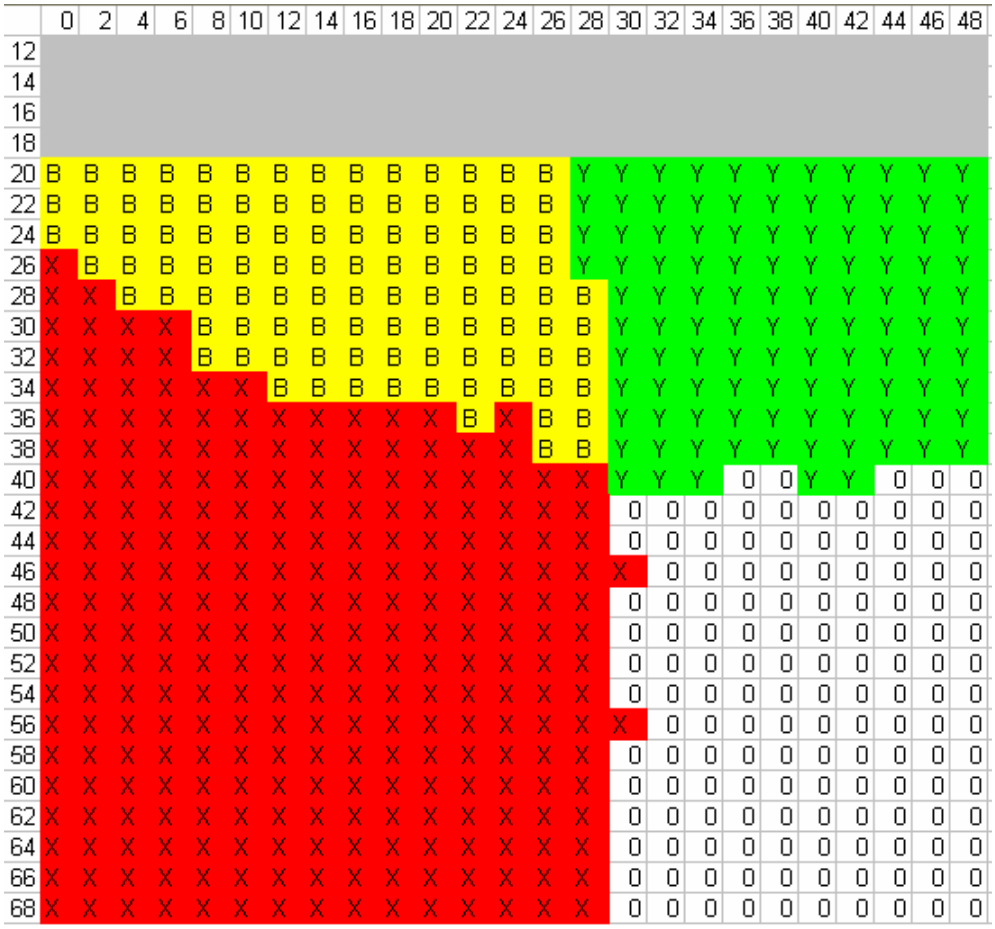

Figure 3.25 16c/deg and 4c/deg spatial frequency components (TP). Same as in figure 3.24

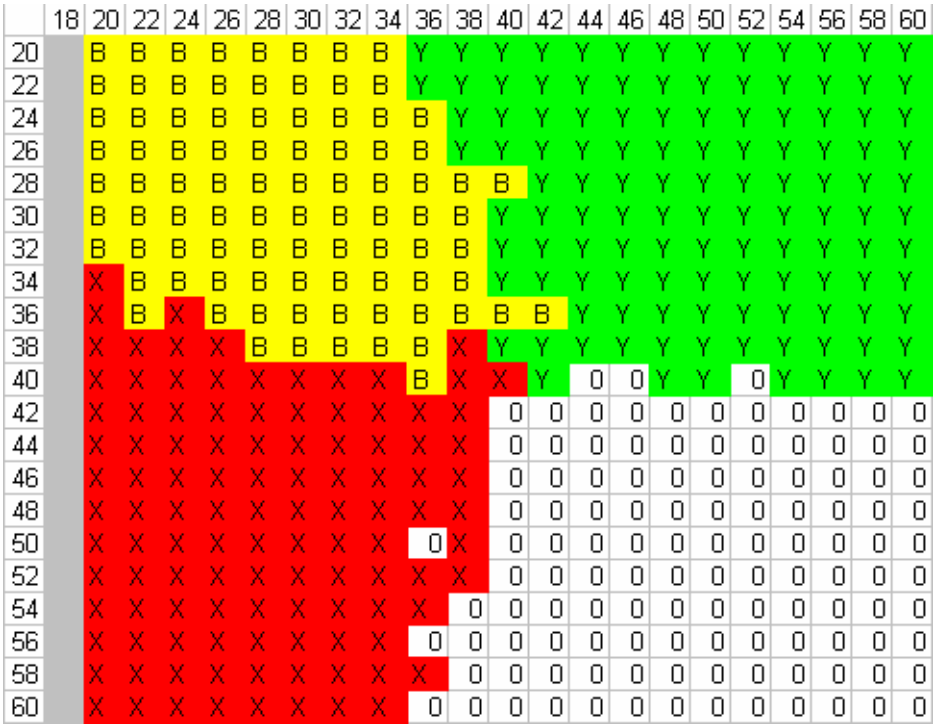

Figure 3.26 6c/deg and 4c/deg spatial frequency components (SP). Same as in figure 3.24

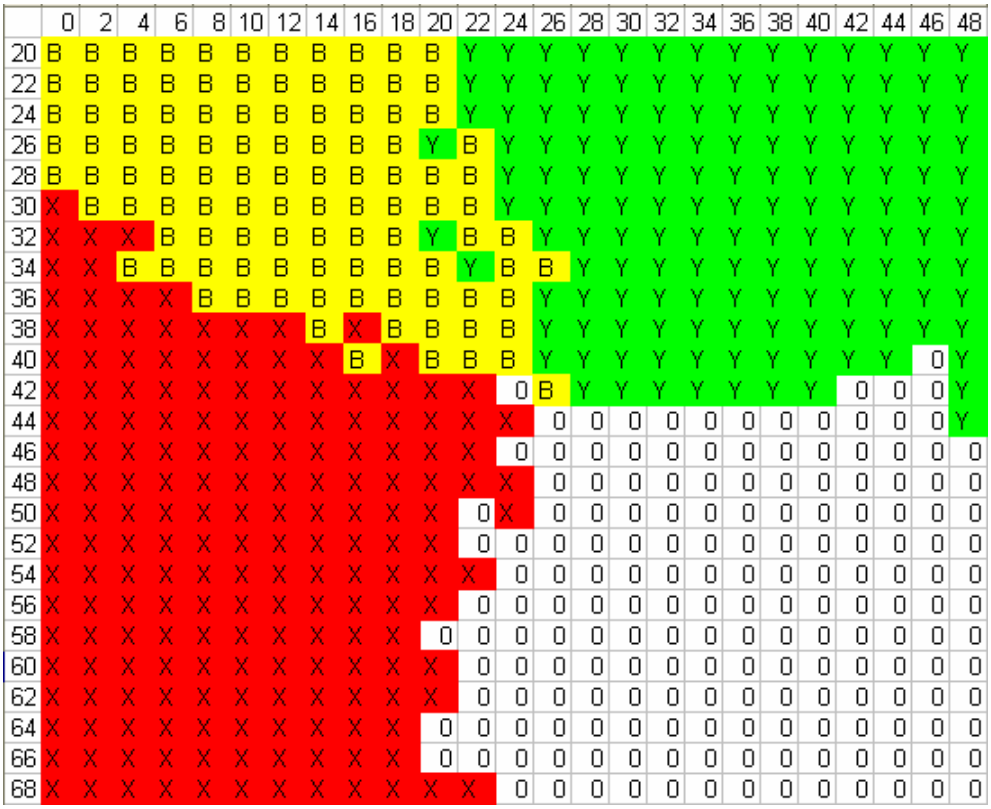

	0	2	4	6	8	10	12	14	16	18	20	22	24	26	28	30	32	34	36	38	40	42	44	46	48
20	B	B	B	B	B	B	B	B	B	B	B	Y	Y	Y	Y	Y	Y	Y	Y	Y	Y	Y	Y	Y	Y
22	B	B	B	B	B	B	B	B	B	B	B	Y	Y	Y	Y	Y	Y	Y	Y	Y	Y	Y	Y	Y	Y
24	B	B	B	B	B	B	B	B	B	B	B	Y	Y	Y	Y	Y	Y	Y	Y	Y	Y	Y	Y	Y	Y
26	B	B	B	B	B	B	B	B	B	B	Y	B	Y	Y	Y	Y	Y	Y	Y	Y	Y	Y	Y	Y	Y
28	B	B	B	B	B	B	B	B	B	B	B	B	Y	Y	Y	Y	Y	Y	Y	Y	Y	Y	Y	Y	Y
30	X	B	B	B	B	B	B	B	B	B	B	B	Y	Y	Y	Y	Y	Y	Y	Y	Y	Y	Y	Y	Y
32	X	X	X	B	B	B	B	B	B	B	Y	B	B	Y	Y	Y	Y	Y	Y	Y	Y	Y	Y	Y	Y
34	X	X	B	B	B	B	B	B	B	B	B	Y	B	B	Y	Y	Y	Y	Y	Y	Y	Y	Y	Y	Y
36	X	X	X	X	B	B	B	B	B	B	B	B	B	Y	Y	Y	Y	Y	Y	Y	Y	Y	Y	Y	Y
38	X	X	X	X	X	X	X	B	X	B	B	B	B	Y	Y	Y	Y	Y	Y	Y	Y	Y	Y	Y	Y
40	X	X	X	X	X	X	X	X	B	X	B	B	B	Y	Y	Y	Y	Y	Y	Y	Y	Y	Y	0	Y
42	X	X	X	X	X	X	X	X	X	X	X	X	0	B	Y	Y	Y	Y	Y	Y	Y	0	0	0	Y
44	X	X	X	X	X	X	X	X	X	X	X	X	X	0	0	0	0	0	0	0	0	0	0	0	Y
46	X	X	X	X	X	X	X	X	X	X	X	X	0	0	0	0	0	0	0	0	0	0	0	0	0
48	X	X	X	X	X	X	X	X	X	X	X	X	X	0	0	0	0	0	0	0	0	0	0	0	0
50	X	X	X	X	X	X	X	X	X	X	X	0	X	0	0	0	0	0	0	0	0	0	0	0	0
52	X	X	X	X	X	X	X	X	X	X	X	0	0	0	0	0	0	0	0	0	0	0	0	0	0
54	X	X	X	X	X	X	X	X	X	X	X	X	0	0	0	0	0	0	0	0	0	0	0	0	0
56	X	X	X	X	X	X	X	X	X	X	X	0	0	0	0	0	0	0	0	0	0	0	0	0	0
58	X	X	X	X	X	X	X	X	X	X	0	0	0	0	0	0	0	0	0	0	0	0	0	0	0
60	X	X	X	X	X	X	X	X	X	X	X	0	0	0	0	0	0	0	0	0	0	0	0	0	0
62	X	X	X	X	X	X	X	X	X	X	X	0	0	0	0	0	0	0	0	0	0	0	0	0	0
64	X	X	X	X	X	X	X	X	X	X	0	0	0	0	0	0	0	0	0	0	0	0	0	0	0
66	X	X	X	X	X	X	X	X	X	X	0	0	0	0	0	0	0	0	0	0	0	0	0	0	0
68	X	X	X	X	X	X	X	X	X	X	X	X	0	0	0	0	0	0	0	0	0	0	0	0	0

Figure 3.27 16c/deg and 4c/deg spatial frequency components (SP). Same as in figure 3.24

There are some interesting points arising from these graphs which would be discussed in the following chapter.

4.0 CHAPTER 4. DISCUSSION – FUTURE WORK

In this chapter the results of the experiment are discussed and compared with previous studies. Also, some future studies are recommended.

4.1 Visibility of compound gratings - Channel interaction at threshold

At this study two experiments were conducted to understand how the multiple spatial frequency channels interact and overlap. In order to achieve this, two experiments screened the threshold performance for compound gratings, approaching the same issue in two different ways.

First, the sensitivity of the compound gratings in two different contrast conditions was tested. The compound gratings were consisted of a primary component at 4c/deg spatial frequency while the spatial frequency of the secondary component was greater by a factor x1.125, x1.25, x1.5, x2, x3, x4 and x6 the spatial frequency of the primary component (i.e. 4.5, 5, 6, 8, 12, 16 and 24c/deg). The two components of the compound gratings were added in two ways: a) having the same contrast threshold b) having a difference in contrast equal to the difference in contrasts found between the threshold of individual spatial frequency components. In all conditions, the observers found to be slightly more sensitive to compound gratings compared to single gratings, when the two components were both projected at their respective threshold. When the spatial frequency of the secondary component was greater than the spatial frequency of the primary component by a factor of x2 (i.e. 4c/deg and 8c/deg components) the mean difference in sensitivity, derived from all subjects, was increased by a factor of x1.15 which means that the sensitivity was increased on average by about 1.2dB. The fact that the difference in sensitivity reaches a plateau for spatial frequency ratio greater than 2 suggests that the interaction between the channels tuned at spatial frequencies of this ratio is less potential and the

sensitivity is increased only due to probability summation. The factor x1.15 is very close to results from other studies about the amount of probability summation between neural channels (Watson 1982; Logvinenko 1993)

Similar results were derived at the second experiment. During this experiment the two components of the compound grating were added for a wide range of contrasts. While the first component was at contrast threshold, the contrast of the other component ranged from sub-threshold to threshold and vice versa. The contrast over the contrast threshold (i.e. relative contrast) of the individual grating was calculated for both components. The relative contrast of the high spatial frequency component was plotted as a function of the low spatial frequency component which always had spatial frequency of 4c/deg. The equation $\left(\frac{C_{m1}}{C^*_{m1}}\right)^a + \left(\frac{C_{m2}}{C^*_{m2}}\right)^a = 1$ fitted to data and the exponent was calculated for every spatial frequency pair. As the ratio of the two components spatial frequencies is getting greater, the value of a was increasing. The value of the exponent ranged from 1.06 to 3.47 (see figure 4.1)

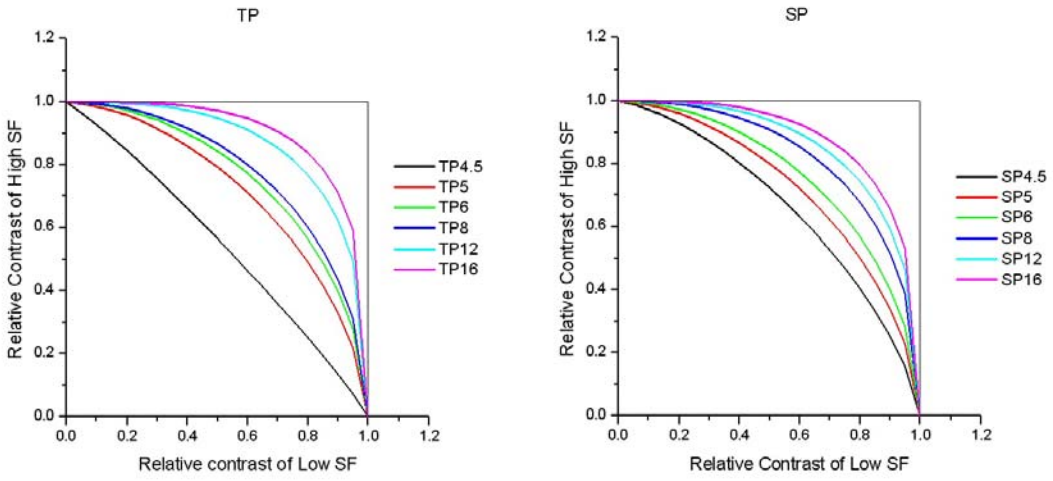

Figure 4.1 Fitted curves for TP (left) and SP (right). The exponent ranges between 1.06 and 3.47. At x and y axis is plotted the relative contrast threshold for the low and the high spatial frequency components, respectively.

The threshold ratio $2^{1/a}$, which is an index of the summation between the two components (and their underlying neuronal channels) was calculated and then plotted as a function of the spatial frequency. The threshold ratio was decreasing as the spatial frequency ratio was getting greater and seems to reach a plateau for ratios greater than 2. This indicates that the interactions between the channels are stronger for ratios less than 2 and weakens for ratios greater than 2. The amount of probability summation calculated from this experiment ranged between x1.265 and x1.345, depending on the equation used for fitting the data.

The results of the current study slightly differ with previous works (Watson 1982) which found that the exponent a ranged between 2.10 and 5.95. But there are some differences between the two works. This work selects a range of spatial frequency pairs laying only from the one side of the CSF peak, which as discussed seems to be mediated from different mechanisms compared the low spatial frequencies. Other studies, used mixing spatial frequency pairs from both sides of the CSF peak, which may affected the values of a. Also, Watson calculated the curves for only one condition, with the components of the compound grating being at equal contrast, while in this work the contrast ratio between the two components occupied a greater range.

4.2 Bandwidth of neuronal channels

Regarding the bandwidth of the spatial frequency tuned channels it must be noted that in this work the bandwidth of a single channel, selective for spatial frequency of 4c/deg was calculated. Previous electrophysiological and psychophysical works found different values for the bandwidth of the spatial frequency selective channels differed a lot depending on the methodological approach. In single striate cortex cell electrophysiological

studies the value of the bandwidth differs from 0.5 to 1.4 octaves(DeValois and DeValois 1990) and in psychophysics experiments from 0.4 to 1.5 octaves ((Blakemore and Campbell 1969; Sachs, Nachmias et al. 1971; Stromeyer and Julesz 1972; De Valois 1977; Watson 1982). In this work the bandwidth of the spatial frequency channel selective in 4c/deg spatial frequency was found to range between 0.36 to 0.59 octaves. The bandwidth was measured at full width half maximum (FWHM) of a Gaussian curve fitted on the data. There is a prominent difference between the technique of previous works and this one. All the other psychophysical experiments measured the bandwidth not for a specific channel (i.e. selective in 4c/deg) but used a range of spatial frequency pairs which occupied many different mechanisms and so an average value of the bandwidth was calculated. It is possible that the bandwidth of the 4c/deg spatial frequency tuned channel is low due to its 'position' at the CSF, i.e. in most subjects a 4c/deg grating shows contrast sensitivity occupying the peak of the CSF. Other neuronal channels may activate more mechanisms. For example, maybe there may be a difference between the bandwidth of the 4c/deg selective channels and another selective at 16c/deg, even though they are measured at the same way. The reason is that the visual system may have more spatial frequency detectors at the peak of the CSF. But all the previous discussion has value under the assumption that the channels are symmetrical at both sides of the CSF.

Some pilot measurements in this work suggest that the spatial frequency channel selective in 4c/deg spatial frequency may be not symmetric. If symmetry exists, then we would expect the exponent a to be similar for spatial frequency ratios 0.25 and 4 and for 0.5 and 2. But all the experimental procedures showed that this is not the case, the 4c/deg spatial selective channel is not symmetric, but asymmetric. If the idea of asymmetry is right, then the bandwidth of the channel is expected to be

greater because the data (see figures 3.22, 3.23) lead to the conclusion that the 4c/deg spatial frequency tuned channel is wider at the low spatial frequency side of the CSF.

4.3 Supra-threshold performance

The results of the second experiment at threshold performance impelled us to continue to the third experiment. While the two components of the compound grating were set at their individual contrast thresholds, some variations appeared either side of the sub-threshold and supra-threshold settings. This indicates that the sub or supra threshold of the one component may affect the detectability of the other, even though the second appears at threshold.

The third experiment was based on pattern discrimination while the contrast of both components laid from sub-threshold to supra-threshold. The observer had to recognize which grating he could see on the screen; one of the two components, the compound grating or nothing.

There are some interesting points regarding the results of this experiment. First of all, the results of the two subjects show similar pattern. Furthermore, at supra-threshold, although the stimulus appears as compound for a wide range of contrasts, it appears that in some cases one component suppresses the visibility of the other. This is more prominent for the component of higher spatial frequency (16 or 6 c/deg), which at supra-threshold is more frequently seen on its own, compared to the 4 c/deg grating. For example, a 6 dB increase in the contrast of the 4 c/deg component requires a 14 dB increase in the contrast of the 16 c/deg component in order for the compound grating to be detected as a single 16 c/deg grating. On the other hand, a 6 dB increase in the contrast of the 16 c/deg component requires a 22 dB increase in the contrast of the 4 c/deg in order for the compound

grating to be detected as a single 4 c/deg grating. This is also the case for the 4 / 6 c/deg compound grating. Concluding, an increasing in contrast of the high spatial frequency component may claim more contrast elevation of the low spatial frequency component to be detected.

4.4 Future work

In the future, more experiments could be undertaken evaluating the threshold ratio while the spatial frequency of the secondary component of the compound grating will be lower than 4c/deg. Accumulating more data from the low spatial frequency side of the CSF will be more accurate to talk about the symmetry or the asymmetry of the spatial frequency channels selective at 4c/deg. Also, it would be interesting if the same experiment will be repeated but having as a centre of the channel a lower and/or a higher spatial frequency, for example 2c/deg and 8c/deg respectively. After these experiments will be more clear if the 'neuronal' channels have the same or different spatial frequency bandwidth depending on the position at the CSF of the main spatial frequency.

The experiments for supra-threshold performance should be continued and a manner of modelling and interpreting these results should be found. There is a possibility that this experiment will allow us to create a 'channelopic' map of the visual system.

References:

Berson, D. M., F. A. Dunn, et al. (2002). "Phototransduction by retinal ganglion cells that set the circadian clock." Science **295**(5557): 1070-3.

Blakemore, C. and F. W. Campbell (1969). "On the existence of neurones in the human visual system selectively sensitive to the orientation and size of retinal images." J Physiol **203**(1): 237-60.

Campbell, F. W. (1968). "APPLICATION OF FOURIER ANALYSIS TO THE VISIBILITY OF GRATINGS." J. Physiol **197**: 551-566.

Campbell, F. W., G. F. Cooper, et al. (1969). "The spatial selectivity of the visual cells of the cat." J Physiol **203**(1): 223-35.

Campbell, F. W. and D. G. Green (1965). "Optical and retinal factors affecting visual resolution." J Physiol **181**(3): 576-93.

Curcio, C. A., K. R. Sloan, et al. (1990). "Human photoreceptor topography." J Comp Neurol **292**(4): 497-523.

De Valois, K. K. (1977). "Spatial frequency adaptation can enhance contrast sensitivity." Vision Res **17**(9): 1057-65.

DeValois, R. L. and K. K. DeValois (1990). "Spatial Vision." Oxford University Press.

Dowling, J. E. and B. B. Boycott (1969). "Retinal ganglion cells: a correlation of anatomical and physiological approaches." UCLA Forum Med Sci **8**: 145-61.

Graham, N. and J. Nachmias (1971). "Detection of grating patterns containing two spatial frequencies: a comparison of single-channel and multiple-channels models." Vision Res **11**(3): 251-9.

Graham, N. and J. G. Robson (1987). "Summation of very close spatial frequencies: the importance of spatial probability summation." Vision Res **27**(11): 1997-2007.

http://hubel.med.harvard.edu.

http://phineasgage.wordpress.com.

http://thebrain.mcgill.ca.

http://webvision.med.utah.edu.

http://wikimedia.org.

Hubel, D. H. (1988). "Eye, Brain and Vision." Scientific American Library.

Kaas, J. H., M. F. Huerta, et al. (1978). "Patterns of retinal terminations and laminar organization of the lateral geniculate nucleus of primates." J Comp Neurol **182**(3): 517-53.

Limb, J. O. and C. B. Rubinstein (1977). "A model of threshold vision incorporating inhomogeneity of the visual field." Vision Res **17**(4): 571-84.

Logvinenko, A. D. (1993). "Lack of convexity of threshold curves for compound gratings: implications for modelling visual pattern detection." Biol. Cybern. **70**: 55-64.

Norton, T. T., D. A. Corliss, et al. (2002). "The Psychophysical Measurement of Visual Function."

Plainis "Unpublished work."

Quick, R. F., Jr., W. W. Mullins, et al. (1978). "Spatial summation effects on two-component grating thresholds." J Opt Soc Am **68**(1): 116-24.
Sachs, M. B., J. Nachmias, et al. (1971). "Spatial-frequency channels in human vision." J Opt Soc Am **61**(9): 1176-86.
Schefrin, B. E., S. J. Tregear, et al. (1999). "Senescent changes in scotopic contrast sensitivity." Vision Res **39**(22): 3728-36.
Stromeyer, C. F., 3rd and B. Julesz (1972). "Spatial-frequency masking in vision: critical bands and spread of masking." J Opt Soc Am **62**(10): 1221-32.
Stromeyer, C. F., III and S. Klein (1975). "Evidence against narrow-band spatial frequency channels in human vision: the detectability of frequency modulated gratings." Vision Res **15**: 899-910.
Tootell, R. B., M. S. Silverman, et al. (1988). "Functional anatomy of macaque striate cortex. V. Spatial frequency." J Neurosci **8**(5): 1610-24.
Watson, A. B. (1982). "Summation of grating patches indicates many types of detector at one retinal location." Vision Res **22**(1): 17-25.
Watson, A. B. and J. Nachmias (1980). "Summation of asynchronous gratings." Vision Res **20**(1): 91-4.
Webster, M. A. and R. L. De Valois (1985). "Relationship between spatial-frequency and orientation tuning of striate-cortex cells." J Opt Soc Am A **2**(7): 1124-32.